UNIVERSITY OF MICHIGAN
JUN 12 1958
PHYSICS LIBRARY
JUN 17 1958

REGISTERED No. M. 3121

PROCEEDINGS

OF THE

INDIAN ACADEMY OF SCIENCES

VOL. XLVII] *SECTION A* [No. 4

APRIL 1958

Price Rs. 2 or 3 Sh. *Annual Subscription Rs. 18*

PRINTED AT THE BANGALORE PRESS, BANGALORE CITY, BY C. VASUDEVA RAO,
SUPERINTENDENT, AND PUBLISHED BY THE INDIAN ACADEMY OF
SCIENCES, BANGALORE

THE OPTIC INTERFERENCE FIGURES OF AMETHYSTINE QUARTZ—PART I

By S. Pancharatnam

(*Memoir No.* 107 *of the Raman Research Institute, Bangalore-6*)

Received April 11, 1958

(Communicated by Sir C. V. Raman)

§1. Introduction

Amethyst is the familiar purple modification of quartz having an absorption band in the yellow-green region of the spectrum, a study of whose optical properties had been reported in an earlier paper.[1] Observations on untwinned amethystine sectors through a polaroid, showed that they exhibited pronounced pleochroism even when observed along the *c*-axis—showing that the *c*-axis was *not* an axis of uniaxial symmetry for the absorption ellipsoid. It followed that the material could not be strictly uniaxial. This was indeed confirmed, though only in the cases of very intensely coloured sectors, was the biaxial nature quite pronounced—the *c*-axis being the acute bisectrix. A sector of this type which was pre-eminently suited for the present study (*i.e.*, which did not possess certain extraneous complicating features characteristic of most quartz-amethyst plates) had been obtained by careful selection during our previous investigation. Of the various conclusions which emerged from that investigation it is sufficient for our present purpose to accept the following particular results, which may be independently deduced from certain observations described in the present paper itself (§§3 and 4):

(*a*) The amethystine sector used is an optically untwinned and genuinely biaxial medium possessing optical activity.

(*b*) The sector is pleochroic, the elliptic section of the absorption ellipsoid normal to the acute bisectrix having its major and minor axes lying respectively parallel and perpendicular to the axial plane.

The optic interference figures displayed in convergent light by this class of media (*viz.*, the class of biaxial media possessing both pronounced pleochroism and optical rotatory power) have not been investigated and are therefore of interest. In the present paper we reproduce and discuss the remarkable types of interference figures exhibited under various conditions by the selected amethystine sector. These interference figures are found to

differ considerably from those displayed both by inactive absorbing crystals and active transparent crystals. It will be shown however that the observations described become explicable in detail in the light of the theory of light propagation in absorbing crystals possessing optical activity; this theory was presented in an earlier paper[2] hereafter referred to as P–*a*. We shall also have frequent occasion to refer to a paper[3] (hereafter referred to as P–IV) where the interference figures of absorbing biaxial crystals had been discussed.

Though it should certainly be possible to repeat our experiments with other deeply coloured sectors of comparable intensity, the impression should not be created that this can be done with any densely coloured area in a basal section of amethyst randomly selected. According to our previous investigation, this is because of certain very interesting—though, from our present point of view, extraneous—complicating factors which feature prominently in most quartz-amethyst plates. In the appendix at the end of Part II, attention is briefly drawn to these complicating factors, and also to the fact that it becomes difficult to compare our results directly with those of other workers.

§2. PRELIMINARY REMARKS

In the present study we have used an intensely coloured amethystine sector occurring in a roughly basal section-plate of the quartz-amethyst about 3 mm. thick. In our previous investigation, an examination of the etch patterns shown by the two surfaces of the plate had revealed that the portion to be used was untwinned and was *right-rotating*, the sector being associated with a secondary rhombohedral face. The tremendous depth of absorption may be estimated from the wedge-spectrograms published in that paper—taken with this coloured area. Because of the large absorption the optic interference figures reproduced in the present paper had to be photographed by focussing a reduced image of a sodium (or mercury) arc directly on the sector using a battery of lenses which also served as the converger. Only an area about 3 mm. square in the body of the sector was used: the remainder of the plate was blackened on both sides with paint to exclude light from adjoining uncoloured and twinned areas. In what follows (particularly in Part II) an acquaintance with the behaviour in convergent light of transparent biaxial crystals—both inactive and active—will be presumed.

§3. OBSERVATIONS IN BLUE LIGHT

Figures 1, 2 and 3 (Plate IX) exhibit the interference figures observed in blue light (λ 4358) at three different settings of *crossed* polaroids. They

prove clearly the biaxial nature of the material, the axial angle for this wavelength being about 8°; the axial plane has been kept horizontal in these photographs—as well as in all the others reproduced in this paper. In Fig. 1 the vibration-directions of the polariser and the analyser lie along and perpendicular to the axial plane while in Fig. 2 they are at 45° to the axial plane. Fig. 3 has been obtained by interchanging the positions which the polariser and analyser occupy in Fig. 2. In these as well as in all other settings of the crossed polaroids it was observed that—unlike the behaviour obtaining in transparent inactive crystals—the optic axial directions were never extinguished; though at the border of the figure the isogyres were fairly dark and appeared at the same position as in non-active crystals, they became diffuse and vanished as the optic axial directions were approached. *This behaviour is characteristic of an ordinary optically active crystal*; and the fact that there is no sensible difference between Figs. 2 and 3 is only what is to be expected for a *transparent* crystal of this class. (This may be shown from reference 4, Eqns. 1 and 2.) In a transparent optically active crystal the optic axial directions may be extinguished by keeping the polariser setting fixed, and rotating the analyser away from the crossed position by an amount equal to the rotation of the plane of polarisation along the optic axial directions. This has been done in Fig. 4, where in addition—purely for achieving a symmetrical interference figure—the polariser and analyser have been adjusted so as to be symmetrically situated with respect to the axial plane. The mean value of the rotation measured in this approximate manner for six azimuths of the polariser was found to be about $-115°$. This being also the rotation for a plate of quartz of the same thickness (*viz.*, 0·28 cm.) the untwinned nature of the medium is again confirmed. (That the material was right-rotating was established—independent of the etch study—by the fact that the rings expanded when the analyser was rotated clockwise).

A curious property not displayed by transparent crystals was however detected. The measured rotation varied systematically with the azimuth of the incident vibration, deviating by as much as ten per cent. from the mean value. This phenomenon will be theoretically explained later (§5); it arises from the fact that the plate is so intensely coloured that even for the blue region of the spectrum the dichroism is not altogether absent, though it is small especially when compared to the optical rotation. Since the latter diminishes with increasing wavelength such effects of dichroism may be expected to be even more prominent for corresponding wavelengths on the long wavelength side of the absorption band. Before proceeding to describe such observations with red light, it is well to confirm also the property

(*b*) mentioned in the introduction: this can be best done by using a wavelength (λ 5890) lying in the heart of the absorption band.

§4. BREWSTER'S BRUSHES

Figure 5 shows the so-called Brewster's brushes as revealed without the use of either polariser or analyser in the unpolarised yellow light of a sodium lamp. It will be seen that they consist of two pairs of brushes, one pair of brushes being associated with each optic axis. For the present we may consider the phenomenon from the elementary standpoint that the behaviour should approximate to that of inactive absorbing crystals as we approach directions represented by points near the border of the field of view. The position of the brushes is in fact the same as exhibited in a crystal such as yttrium platinocyanide[5] which has a small axial angle and is inactive.

In non-active crystals Brewster's brushes will be seen only when there is pronounced dichroism along the optic axial directions; and they will then lie along zones for which the principal planes of linear birefringence are inclined at 45° to the principal planes of linear dichroism. In the present case the brushes are seen to lie along the same zone as the isogyres of the biaxial interference figure when the polariser and analyser are at 45° to the axial plane (refer *e.g.* Fig. 2). This means that the principal radii of the elliptic section of the absorption ellipsoid (taken normal to the acute bisectrix) lie along and perpendicular to the axial plane, *i.e.*, along $O'X_k$ and $O'Y_k$ in Fig. 1, text, of Part II: this diagram represents the field of view of the convergent light figure, O′ representing the acute bisectrix, while O_1 and O_2 represent the two optic axes.

Which of the directions $O'X_k$, $O'Y_k$ correspond to the less absorbed vibration in the absence of optical activity could be determined in the following manner. The plate was tilted first about a horizontal axis (so as to effectively eliminate the effects of optical activity) and the depth of absorption for the horizontal vibration direction was noted in *parallel* light. An analogous procedure was adopted for observing the depth of absorption for a vibration parallel to $O'Y_k$; this was seen to be enormously greater than that for the vibration $O'X_k$, thus independently confirming the statement (*b*) made in the introduction.

Though the explanation of Brewster's brushes given in this section appears to have completely neglected the presence of optical activity, it actually holds to a higher degree of approximation than is to be suspected from such a statement. According to P–*a*, §7 *b*, we may—for directions not too close to an optic axis—neglect the *squares* of the ellipticity of the waves

(and hence the square of the non-orthogonality factor cos $\frac{1}{2}c$) even though the first power of these quantities may not be negligible. For such directions it has also been shown that the absorption coefficients of the waves propagated along any direction will be virtually the same as in the absence of optical activity. Referring now to Eqn. (11) of P–IV it follows that the intensity at any point in the field seen directly in unpolarised light will be the same as in an inactive crystal (neglecting the squares of the ellipticity of the waves, in both cases). Hence the explanation of Brewster's brushes as customarily presented for an inactive absorbing crystal (Pockels,[6] p. 424) may be also applied in the present case—(*see* also Part II, §7).

In the present paper *we shall be making the following approximation* which is quite customary, *viz.*, that the elliptic section of the absorption ellipsoid made by the plane of the paper in Fig. 1, text, Part II, is practically the same (in orientation and dimension) as the section normal to any direction of propagation in the angular range considered. [That this approximation is not strictly true is shown by the asymmetry of the intensity of Brewster's brushes with respect to the axial plane (*see* Appendix)]. For the purpose of our qualitative discussion we shall also take the rotatory power to be constant over the range of directions under consideration.

§5. Observations in Red Light

Figures 6, 7 and 8 (Plate X) show the biaxial interference figures exhibited in red light (6450–6900 Å) at three different settings of *crossed* polaroids which correspond respectively to the three settings already used in Figs. 1, 2 and 3 with blue light. Apart from the very appreciable increase of the axial angle (relative to blue light), the most striking feature is that Figs. 7 and 8 are *not* identical since the brush apparently goes through the eyes in the latter. Any such alteration in the interference figure caused by a mere interchanging of crossed polaroids implies that the waves propagated along a general direction are in two general non-orthogonally polarised states, and that *the relation between these states of polarisation is necessarily different from that obtaining in inactive absorbing crystals* (*see* P–IV, §8 *a*).

It was observed that in the setting of Fig. 8—for which the vibration-direction of the polariser is inclined at $-45°$ with respect to the axial plane—the portion of the brush which apparently passes through the eyes was really not perfectly dark; and that the optic axial directions could be more perfectly extinguished by turning the analyser clockwise, away from the crossed position, through a small angle—the mean value of this angle for obtaining best extinction being estimated to be 31°. On the other hand when the vibration-direction

of the polariser made an angle of $+45°$ with respect to the axial plane (as in Fig. 7), the analyser had to be turned (from the crossed position) through the much larger angle of 50° to reach a position where the optic axis appeared best extinguished. For any general setting of the polariser the axial directions can be extinguished by a similar procedure, as illustrated in Fig. 9 (where, in addition, the polariser and analyser have been oriented symmetrically with respect to the axial plane).

Along an axial direction in a *transparent* active crystal two oppositely polarised circular vibrations are propagated with 'circular birefringence' $|2\rho|$. In the present case such a supposition cannot account for the phenomenon noted in the previous paragraph—which had also been exhibited less conspicuously in blue light, *viz.*, the variation of the apparent rotation with the azimuth of the incident vibration. But in P–*a*, §8 *a*, it had been theoretically deduced that in an optically active crystal with weak linear dichroism ($k < |2\rho|$) the waves propagated along an axial direction will be *elliptically* polarised: the two elliptic vibrations will be exactly similar in form and orientation but will be described in opposite senses. The major axes of the ellipses will be coincident and—since the rotatory power is negative in the present case—will make an angle of $-45°$ with respect to the line $O'X_k$ (Fig. 1, text, Part II) which is the trace of the axial plane as well as the trace of a principal plane of linear dichroism.

Before proceeding further we shall describe an experiment confirming the theoretical results stated in the last paragraph. The crystal was as usual kept in the conoscopic arrangement between crossed polaroids which could be turned around *together*; but a mica retardation plate was set immediately behind the first polaroid and an *identical* retardation plate was set immediately in front of the second polaroid with its principal planes turned round by 90° with respect to the first. The two retardation plates were coupled so that they could be turned around *together*. The arrangement in front of the crystal constitutes an '*elliptic polariser*'. The arrangement behind the crystal constitutes a '*crossed elliptic analyser*' which, if the crystal plate were absent, would *automatically* cut out the elliptically polarised light produced by the arrangement in front—independent of the setting of the coupled polaroids and the coupled retardation plates. In the present case, $\lambda/4$ retardation plates were used, the principal planes being oriented at an angle of 45° to the axial plane. Thus the principal axes of the incident elliptic vibration were equally inclined to the axial plane, though the ellipticity could be altered by turning the coupled polaroids. It was observed that there were two settings of the coupled polaroids at which the optic axial

directions were extinguished—the figure for one of these settings being reproduced in Fig. 10. These were the two settings at which the vibration-direction of the first polaroid made angles of + 34° and − 34° with respect to O'M (Fig. 3 *b*, text, Part II) as roughly determined by the fact that the spots had moved exactly into the axial plane at these settings. *This confirms that the two waves propagated along each optic axis are elliptically polarised* as described above—the numerical value of the ellipticity $|\omega|$ of both vibrations being about 34°. On the Poincaré sphere (Fig. 1, text), the states of polarisation of these two waves are denoted by the points A and B lying on the same meridian of longitude but at latitudes -2ω and $+2\omega$ respectively.

The variation of the measured rotation with the azimuth of the incident vibration may now be understood by applying the results of ref. 7, §§4 and 5, for discussing the dissolution of the incident vibration into two elliptic vibrations, and the compounding of the latter after their propagation through the plate with different velocities but equal absorption coefficients. The actual rotatory power along an axial direction can in fact be calculated from the apparent rotations a_1 and a_2 observed with the incident vibration lying respectively parallel and perpendicular to the major axes of the elliptic vibrations propagated. Considering first the former case the incident vibration will be represented on the Poincaré sphere by the point M on the equator (Fig. 1, text, Part I). It will be decomposed into two vibrations in states A and B whose intensities will be equal and whose initial ' phase difference ' will be zero since M lies on the arc AB (reference 7, §4). Hence if the slower wave B suffers a phase retardation of ϕ relative to the other on propagation through the plate along an axial direction, then ϕ also represents the absolute phase advance of vibration A over B when they emerge from the plate. These vibrations will still be of equal intensity—their absorption on passage through the plate being equal according to P–*a*, §8 *a*—so that they will compound to give a *linear* vibration represented by a point C_1 on the equator (reference 7, §5); if E_1' be the area of the triangle $C_1'BA$, where C_1' is the point opposite to C_1, then $\frac{1}{2}E_1'$ should be equal to the supplement of the absolute phase advance of vibration A over B (*see* reference 7, Eq. 5 *b*). The spherical excess $\frac{1}{2}E_1'$ of the right-angled triangle $C_1'BM$ may be obtained from spherical trigonometry:

$$\tan \tfrac{1}{2}E_1' = \tan \omega \tan \tfrac{1}{2}(\pi - 2a_1).$$

Hence

$$\cot \tfrac{1}{2}\phi = \tan \omega \cot a_1 \qquad (1)$$

On the other hand, if the incident vibration is turned to the orthogonal state M′, the two vibrations into which it is split along an optic axial direction will have an initial phase difference of $-\pi$ and a final phase difference

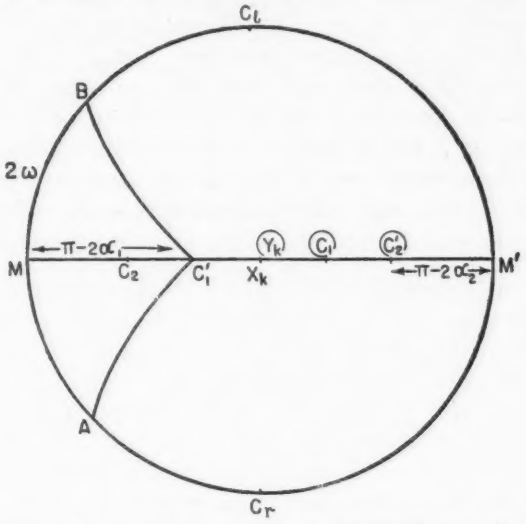

TEXT–FIG. 1. The Poincaré sphere as used for explaining the apparent variation of optical rotation with the azimuth of the incident vibration. Symbols enclosed in circles represent points on the hemisphere below the plane of the paper.

of $(\phi - \pi)$, compounding finally to give the linear vibration in state C_2. Hence if C_2' represent the state orthogonal to C_2, then ϕ should be equal to half the spherical excess of the triangle $C_2'AB$. Proceeding as before we get from spherical trigonometry,

$$\tan \tfrac{1}{2}\phi = \tan \omega \tan \alpha_2 \qquad (2)$$

From (1) and (2) we obtain

$$\tan^2 \omega = \frac{\tan \alpha_1}{\tan \alpha_2} \qquad (3)$$

$$\tan^2 \tfrac{1}{2}\phi = \tan \alpha_1 \tan \alpha_2 \qquad (4)$$

The apparent rotations α_1 and α_2 observed in the respective cases when the incident vibration lies parallel to O′M and O′M′ (Fig. 3 *b*, text, Part II) have been roughly measured to be 31° and 50° respectively (refer above). Inserting these values in (3) and (4) we find firstly that the numerical ellipticity $|\omega|$ of the vibrations propagated along an optic axis should be 35·5°—in

FIG. 1

FIG. 2

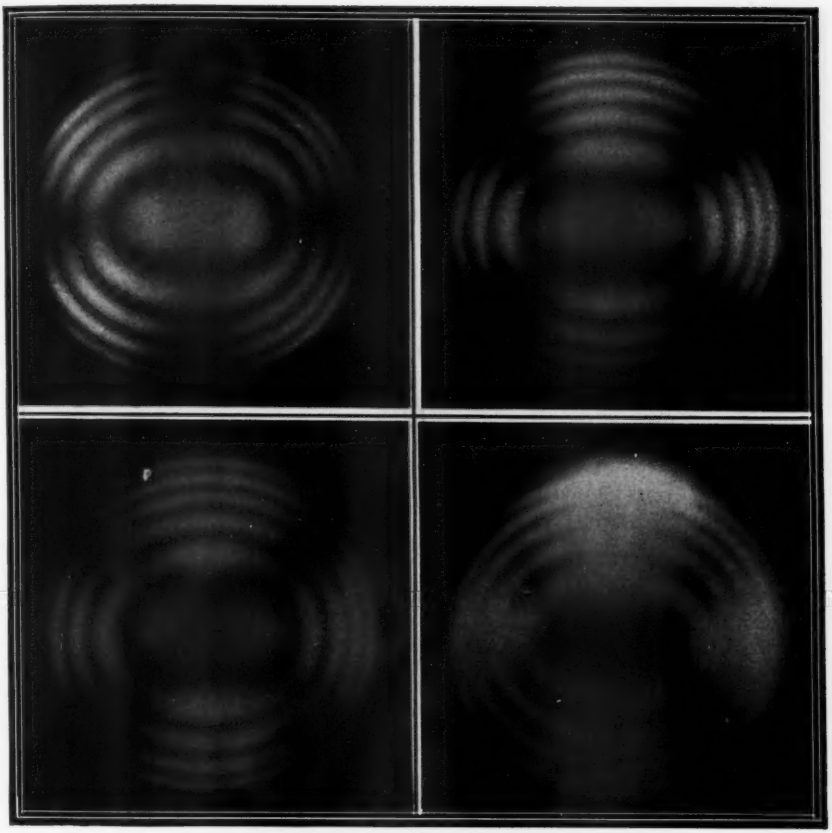

FIG. 3

FIG. 4

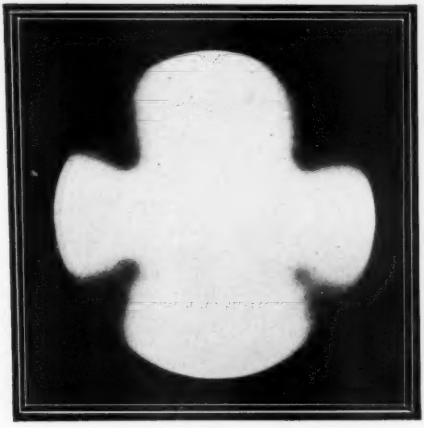

FIG. 5

FIGS. 1-5

FIG. 6

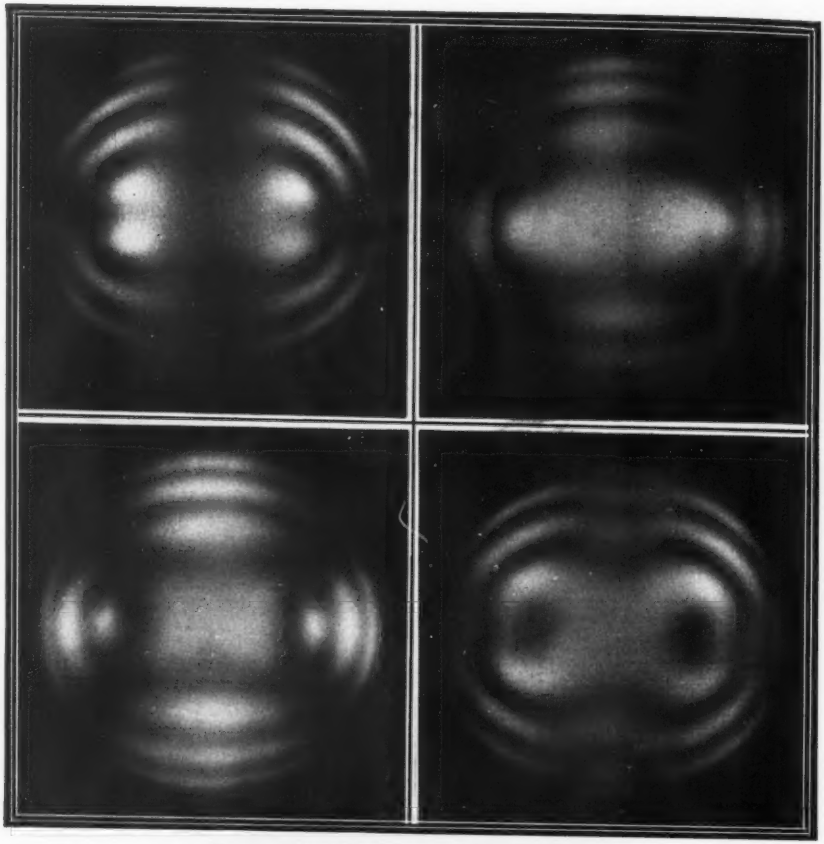

FIG. 7

FIG. 8

FIG. 9

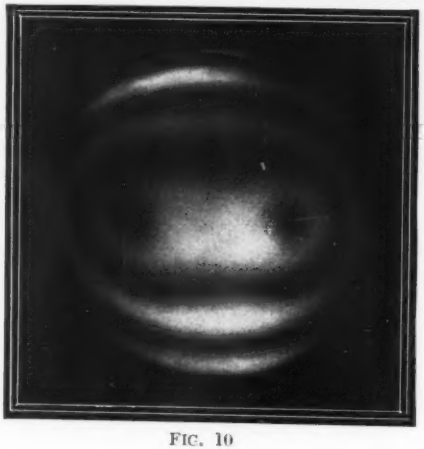

FIG. 10

FIGS. 6–10

agreement with the experimentally estimated value of 34°, previously quoted; secondly, the relative phase advance ϕ gained by the faster wave over the slower wave on passage through the plate is found to be 80·5°. Since the waves are not circularly polarised, the relative phase difference per unit path (ϕ/d) is *not* directly equal to $|2\rho|$ but is related to it by Eq. (17) of P–*a*:

$$|\rho| d = \frac{\frac{1}{2}\phi}{\sin|2\omega|} \tag{5}$$

The true optical rotation $|\rho| d$ which would be exhibited by the plate in the absence of dichroism may be calculated from (5) by substituting the values of ω and ϕ obtained from (3) and (4). In the present case it is found to be 42·5°. (Though this is somewhat lower than the optical rotation for a plate of transparent quartz, the difference may be entirely due to the large experimental errors involved).

§6. Summary

The interference figures exhibited by an intensely coloured amethystine sector at two wavelengths which lie practically outside the absorption band are reproduced. In blue light the interference figures are characteristic of a transparent biaxial crystal possessing the rotatory power of quartz. In red light the axial angle is larger, and effects due to weak linear dichroism are also exhibited. Thus the rotation of the plane of polarisation along the optic axes varies with the azimuth of the incident vibration; and the method of determining the rotatory power from the apparent rotation is illustrated.

§7. References

1. Pancharatnam .. *Proc. Ind. Acad. Sci.*, 1954, **40 A**, 196.
2. ———— (P-*a*) .. *Ibid.*, 1957, **46 A**, 280.
3. ———— (P-IV) .. *Ibid.*, 1957, **45 A**, 2.
4. ———— .. *Ibid.*, 1957, **45 A**, 402.
5. Boguslowski .. *Ann. der Physik*, 1914, **44**, 1084.
6. Pockels .. *Lehrbuch der Kristalloptick*, *Teubner*, 1906.
7. Pancharatnam .. *Proc. Ind. Acad. Sci.*, 1956, **44 A**, 247.

THE OPTIC INTERFERENCE FIGURES OF AMETHYSTINE QUARTZ—PART II

By S. Pancharatnam

(*Memoir No. 107 of the Raman Research Institute, Bangalore-6*)

Received on April 9, 1958

(Communicated by Sir C. V. Raman)

§1. Introduction

In the remaining part of the paper, observations on the interference figures of the amethystine sector are continued, using a wavelength lying in the heart of the absorption band (λ 5890). Here the effects of dichroism gain such ascendancy ($k > 2 \mid \rho \mid$) that the existence of optical rotatory power is itself only indirectly manifested—through the exceptional nature of the observed phenomena.

§2. Observations between Crossed Polaroids

Figures 1–6 (Plate XI) demonstrate the singular behaviour of the isogyres observed between *crossed* polaroids as the latter are turned around *together* in a clockwise sense—starting with the setting in which the vibration-direction of the polariser is parallel to the axial plane. (The settings of polariser and analyser have been respectively marked in the upper and lower circles drawn by the side of each figure, the axial directions themselves being marked by white dots in some of the photographs.) *There are only two settings of the incident vibration, viz.*, when it is parallel to either $O'A_1$ or $O'A_2$ in Fig. 1, text, *for which genuine isogyres are observed* passing unmodified through the two optic axes, as seen in Figs. 2 and 3 (Plate XI). For all other settings of the crossed polaroids it was observed that the 'isogyres' appeared really dark only towards the border of the figure. This is true even in Figs. 5 and 6 though the crossed polaroids are in orientations obtained merely by interchanging the polariser and analyser in the settings of Figs. 2 and 3 respectively.

§3. Properties of the Optic Axes

The observations of the previous paragraph clearly mean that when the incident vibration is parallel to either $O'A_1$ or $O'A_2$ (Fig. 1, text) it is propagated without resolution along each axial direction. We thus arrive experimentally at the conclusion that *the waves propagated along an optic axis, e.g.*, along O_1, *are linearly polarised along two non-orthogonal directions*

parallel to $O'A_1$ and $O'A_2$, as marked at O_1 in Fig. 1, text. These directions are found to be equally inclined to the lines bisecting the angle between $O'X_k$ and $O'Y_k$, and lie in the negative quadrant. These results are exactly what have been already derived* theoretically in P–a^1, §8 *b*, for the propagation along an axial direction when the dichroism is sufficiently large ($k > |2\rho|$). For the purpose of discussion it is convenient to refer to Fig. 2 *a* text, which represents a plate cut exactly normal to an optic axis on which have been marked the principal planes of linear dichroism OX_k and OY_k. The linearly polarised states P_a and P_b of the waves that can be propagated normal to the plate should both lie in the negative quadrant (since ρ is negative) at azimuths whose numerical values ψ_1 and $(\frac{1}{2}\pi - \psi_1)$ are the roots of

$$\tfrac{1}{2}k \sin 2\psi = |\rho| \tag{1}$$

Furthermore, these waves should differ not in their velocities, but only in their coefficients of absorption k_a and k_b:

$$(k_b - k_a) = k \cos 2\psi_1 \tag{2}$$

When the vibration incident along an axial direction is in a general setting (*i.e.*, other than $O'A_1$ or $O'A_2$), it will be decomposed into two non-orthogonal vibrations in states P_a and P_b according to the parallelogram law (*see e.g.*, reference 2, Fig. 3); while according to the same law the attenuated vibrations emerging from the plate should compound to yield a linear vibration whose azimuth would have turned towards the plane of the less attenuated state P_a. In accordance with this it was always found possible to extinguish the optic axial directions by turning the analyser away from the crossed position. This is illustrated in Figs. 7 and 8 (Plate XII); in Fig. 7 the angles that the vibration-directions of the polariser and analyser made with respect to $O'X_k$ were $-59°$ and $+59°$ respectively; while for Fig. 8 the corresponding angles were $-84\frac{1}{2}°$ and $+84\frac{1}{2}°$. A straightforward calculation—based on the explanation given above of the extinction of the optic axes—enables the difference in the absorption coefficients of the waves propagated along an axial direction to be estimated. If d be the thickness of the plate, it is easily shown that for an axial direction $(k_b - k_a)\,d$ is equal to 2·5, this being the mean of the two values calculated from the settings of Figs. 7 and 8 respectively. The angle between $O'A_1$

* These results may also be derived analytically by directly applying the principle of superposition. Thus, if both sides of (1) be multiplied by dz, the left-hand side and right-hand side denote respectively the angles through which a plane vibration at azimuth ψ turns during the infinitesimal operations of dichroism and rotation respectively; for these to be equal and opposite, eq. (1) should be satisfied, and the plane of vibration should lie in the negative quadrant, if ρ is negative.

and $O'A_2$ (*i.e.*, between the settings of the polariser in Figs. 2 and 3) was required in the calculation; it was estimated to be 50°, this being done more accurately from observations using a polariser alone and an analyser alone (§8). (It may be noted that this angle may also be *calculated* by measuring the turning of the plane of polarisation along the axial directions for *two* azimuths of the incident vibration, as in Figs. 7 and 8.) We then obtain $kd = 3{\cdot}25$ from (2), giving an estimate of the 'pure' linear dichroism.

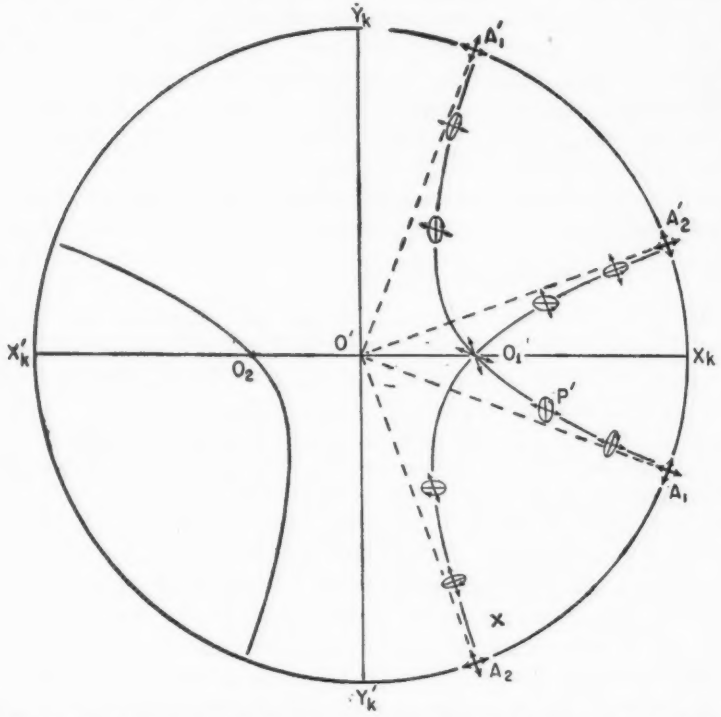

TEXT-FIG. 1. Convergent light figure depicting the variation of the states of polarisation of the waves with the direction of propagation for particular zones in the field of view. O_1 and O_2 are the optic axes.

The optical rotatory power along the axial directions—though masked by the effects of dichroism—may now be indirectly estimated by substituting the values $\psi_1 = 20°$, and $kd = 3{\cdot}25$ in (1). The total optical rotation $|\rho|\,d$ (which would be exhibited along the axial directions in the absence of dichroism) turns out to be about 59·5°—after conversion from radians to degrees. Since this is practically the same as the rotation for a plate of transparent

quartz of the same thickness (*viz.*, 2·8 mm.), we have here a semi-quantitative check on the results of our theory.

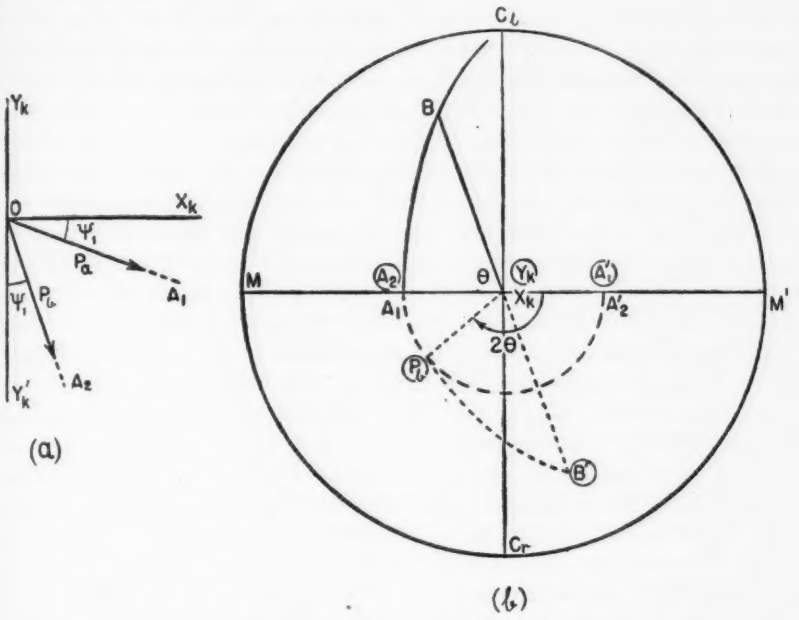

TEXT–FIG. 2. (*a*) Plate cut normal to an optic axis along which the waves propagated are linearly polarised in non-orthogonal states P_a and P_b.

(*b*) Construction on the Poincaré sphere determining the points A_1 and P_b which represent the states propagated unchanged along the direction P′ of Fig. 1, Text.

§4. Explanation of the Formation of Isogyres

We now turn to the fact that in Fig. 2 for example—where the vibration-direction of the polariser is parallel to $O'A_1$ (Fig. 1, text)—it is not the two optic axial directions *alone* that are extinguished; all the directions represented by points on the dark isogyres are extinguished (in sharp contrast to the behaviour of transparent active crystals). These isogyres form a rectangular hyperbola (with $O'A_1$ and $O'A_1'$ as asymptotes) one branch of which has been marked $A_1O_1A'_1$ in Fig. 1, text. We may conclude from our observation that along any direction represented by a point on this hyperbola (*e.g.*, the point P′), a vibration parallel to $O'A_1$ can be propagated unchanged—so as to be completely extinguished by the crossed analyser; while for the same direction P′ a vibration parallel to $O'A_1'$ is *not* propagated

unchanged—as is shown by the absence of isogyres in Fig. 5, obtained by interchanging the polariser and analyser settings of Fig. 2.

This conclusion may be theoretically explained by the method of superposition presented in P–*a*: for a general direction of propagation we will observe the superposed effects not only of linear dichroism and optical rotation (as along the axial directions) but also of the linear birefringence which would be present even in a transparent inactive crystal. The clue to the explanation of the isogyres which form when the vibration-direction of the polariser is parallel to $O'A_1$ (Fig. 1, text) is given by the fact that the isogyres (one branch of which is marked $A_1O_1A_1'$) would have occurred in the same position even in the absence of optical activity and linear dichroism (*see e.g.*, Johannsen[3]). That is to say, any point such as P′ lying on these isogyres represents a direction for which one of the principal planes of linear birefringence lies parallel to $O'A_1$. Hence, for such a direction a vibration parallel to $O'A_1$ will remain unchanged under the effect of the infinitesimal operation of linear birefringence. The same vibration will also remain unaltered under the *combined* effects of the two succeeding infinitesimal operations of linear dichroism and optical rotation—as is evidenced by the fact that it is propagated unchanged along the axial directions where these two factors alone subsist (§3). It follows that a vibration parallel to $O'A_1$ can be propagated unaltered (along the zone of directions represented by the isogyres) under the combined effect of all three factors, *viz.*, linear birefringence, linear dichroism and optical rotation. It may be similarly proved that a vibration parallel to $O'A_1'$ cannot be propagated unchanged along these directions; for it is *not* propagated unchanged under the combined effects of the second two factors alone—as is evidenced by the fact that it is not propagated unchanged along an axial direction. This explains the presence of genuine isogyres in Fig. 2 and their absence in Fig. 5.

The isogyres in Fig. 3 form a rectangular hyperbola—with asymptotes $O'A_2$ and $O'A_2'$—one branch of which has been marked $A_2O_1A_2'$. It may be shown by an exactly similar argument that along the zone of directions represented by this hyperbola a vibration parallel to $O'A_2$ can be propagated unchanged, but not a vibration parallel to $O'A_2'$; this explains the presence of genuine isogyres in Fig. 3 and their absence in Fig. 6.

The main result of this section may be summarised in a form applicable to crystals of arbitrary axial angle and of any symmetry (in a region where $k > |2\rho|$). *Isogyres are formed between crossed polaroids only when the polariser setting is parallel to one of the vibration-directions of the waves propagated along an optic axis*; the isogyres then occupy the same position

as they would in a transparent inactive crystal with the same axial directions. It is, of course, assumed that the optical rotatory power and linear dichroism do not vary rapidly in the neighbourhood of the optic axis considered.

§5. States of Polarisation of the Waves

(*a*) *Co-ordinates for points in convergent light figure.*—We shall now see what will be the states of polarisation of the waves propagated along the direction represented by the arbitrary point P in the convergent light figure (Fig. 3 *a*, text). In the present case, it is best to specify the point P in curvilinear co-ordinates δ, χ. In the region of view in Fig. 3 *a*, text, we can draw two families of intersecting curves. The point P has been depicted as the point of intersection of two of these curves. The first is a curve of constant linear birefringence characterised by the parameter δ which is equal to the linear birefringence, *i.e.*, the birefringence in the absence of optical activity and linear dichroism; this curve takes the form of an 'oval of Cassini' (*see e.g.*, Wooster[4]). The second curve is a branch of a rectangular hyperbola which is drawn passing through the two optic axes, having as its asymptotes two perpendicular lines O'L and O'L' drawn through the centre of the figure. This hyperbola really represents a curve of like polarisation in the absence of optical activity and linear dichroism, since it would then represent the position of the isogyres formed when the crossed polaroids are set parallel to O'L and O'L' (*see* Johannsen[3]). The hyperbolic segment O_1PL may be characterised by the parameter χ, where $(-\chi)$ is the angle that its asymptote O'L makes with respect to $O'X_k$. For any point on this hyperbolic segment χ the principal plane of linear birefringence OX_r (corresponding to the slower wave in the absence of optical activity and dichroism) makes an angle $-\chi$ with $O'X_k$.

For a point in the convergent light figure which is related to P by inversion about the central point O', the orientation of the principal planes of linear birefringence, as well as the magnitude of the linear birefringence will be the same as for the point P itself. All other factors being taken to be constant over the field of view, *the interference figures in convergent light must always be centrosymmetric about O'*. That this is not strictly what is observed (*see e.g.*, Brewster's brushes, Part I, Fig. 5, Plate IX) is mainly because the coefficients of linear dichroism exhibit some variation over the field of view. For the sake of our qualitative discussion we may neglect this variation. Accordingly *it is sufficient to consider only the field of view on the right of the vertical line* Y_kY_k'.

(*b*) *Approximate discussion.—For directions of propagation lying towards the border of the figure*, the variation of the states of polarisation of the two

waves as we proceed round a curve of constant linear birefringence δ may be easily studied in a fairly comprehensive manner. The two waves propagated along the direction P will be elliptically polarised; and according to the approximate results of P–a[1], §7 b, we may take the major axes of the

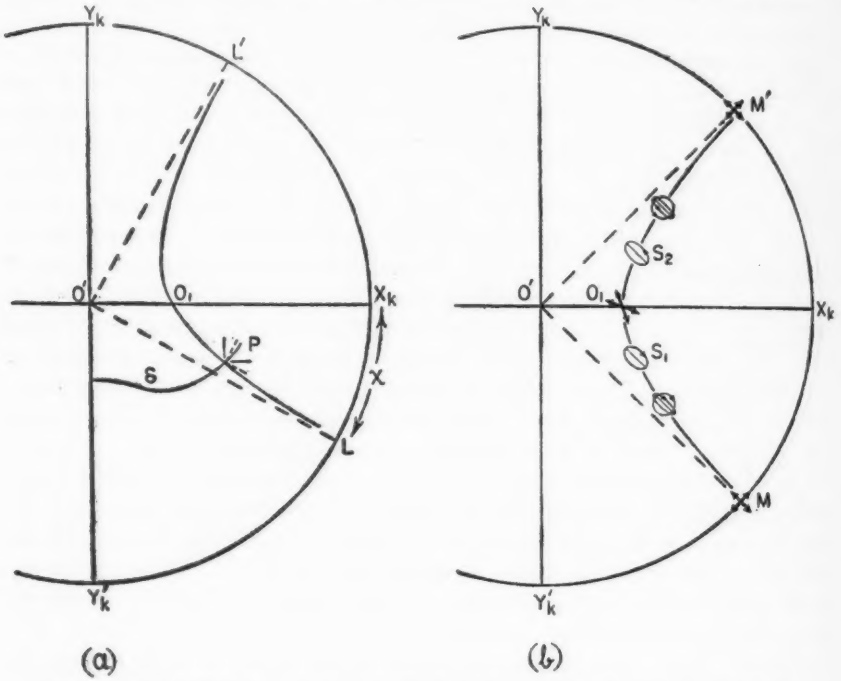

TEXT–FIG. 3. (a) Curvilinear co-ordinates (δ, χ) for the point P in the convergent light figure. (b) States of polarisation of the waves propagated along directions represented by points on MO_1M'; S_1 and S_2 are the singular axes.

slower and faster ellipses to lie along the corresponding principal planes of linear birefringence (OX_τ and OY_τ); and if ω represent the ellipticity of one of these elliptically polarised waves propagated along P (δ, χ), then since ρ is negative in the present case,

$$\omega = \pm\,|\rho|\,/\delta - \tfrac{1}{2}k \sin 2\chi/\delta \qquad (3)\dagger$$

the first term being taken with a positive or negative sign according as the ellipticity of the slower or faster wave is required.

† We had inadvertantly omitted, in P–a, eq. 15, to include a negative sign before the expression for ϵ, the common ellipticity of the waves in the absence of optical activity.

The variation of the ellipticity of the waves with direction (for points near the border of the figure) may be obtained from (3). We shall not proceed to describe this variation, since for such directions, the ellipticity is so small, that any experimental test using elliptically polarised light becomes difficult. It is to be noted that (3) may also be used for discussing the propagation for wavelengths in the red (where $k < |2\rho|$). But a characteristic difference which arises only in the present case (where yellow light is used) may be mentioned: there exists a zone of directions, *viz.*, those included between the segments O_1A_2 and O_1A_1 as also those between O_1A_2' and O_1A_1', for which both ellipses have the same sense of description—this common sense of description being the same as that in an inactive absorbing crystal.

(*c*) *General direction of propagation.*—The principal planes of linear birefringence and linear dichroism corresponding to the direction P have been marked at P itself in Fig. 3 *a*, text, while they have also been marked in P–*a*, Fig. 1 *a*, for a plate cut normal to the direction represented by P. The states of elliptic polarisation of the waves propagated along the general direction P (δ, χ) may now be accurately determined using the results proved in P–*a* which we may briefly recapitulate.

The horizontal and vertical directions will be represented on the Poincaré sphere by two opposite points X_k and Y_k on the equator—the diameter $X_k Y_k$ being kept perpendicular to the paper in our diagrams. From the theory for transparent active crystals we may regard as given (*a*) the elliptic birefringence Δ in the absence of dichroism, (*b*) the diametrically opposite points B and B′ which represent the states of elliptic polarisation of the slower and faster waves propagated along the direction P in the absence of dichroism (*vide* P–*a*, Fig. 2 and §3 *a*). The states of polarisation of the waves actually propagated in the direction P (*i.e.*, with linear dichroism present) will be represented on the Poincaré sphere by two points P_a and P_b which we wish to determine. Now the angular distances $2\psi_a$ and $2\phi_a$ of the slower state P_a from X_k and B are also the angular distances of P_b from the opposite points Y_k and B′; and further, P_a and P_b lie on the same side of the great circle passing through X_k and B—the hemisphere on which they lie being fixed by the fact that the vertices B, P_a and X_k describe the triangle BP_aX_k in a positive sense. Because of this relation it becomes sufficient to locate geometrically the position of P_a; this may be done from the following additional features regarding the triangle BP_aX_k; (*i*) the angle at P_a is a right angle; (*ii*) the ratio of the sines of the angular distances $2\phi_a$ and $2\psi_a$ of P_a from B and X_k is equal to k/Δ. The absorption

coefficients and refractive indices of the states P_a and P_b are given by P-*a*, Eqns. 9 and 12.

The region of the convergent light figure which need be theoretically studied is considerably reduced by the following relation which may be proved from the results of P-*a*. The points on the Poincaré sphere, representing the states of polarisation of the waves propagated along the direction $P(\delta, \chi - \frac{1}{2}\pi)$ are obtained from those representing the states propagated along $P(\delta, \chi)$, by reflection about the equatorial plane of the sphere: the refractive indices of the states are interchanged after reflection but not the absorption coefficients. So also the points on the Poincaré sphere representing the states propagated along $P(\delta, \frac{1}{2}\pi - \chi)$ may be obtained from those representing the states propagated along $P(\delta, \chi)$ by reflection about the plane C_lMC_r: the absorption coefficients of the states are interchanged after reflection but not the refractive indices. We shall proceed to apply the results quoted in this sub-section to discuss in detail the propagation along particular zones of directions.

§6. OBSERVATIONS WITH ELLIPTICALLY POLARISED LIGHT

Let us now consider a direction of propagation such as P′ lying on the hyperbolic segment O_1A_1 (Fig. 1, text). For such a direction the principal plane of linear birefringence OX_r lies parallel to $O'A_1$ and is represented on the Poincaré sphere by the point A_1 on the equator (*see* Fig. 2 *b*, text). The point B representing the state of polarisation of the slower wave in the absence of absorption, will lie on the meridian A_1C_l—since this state will be left-elliptically polarised with its major axis parallel to $O'A_1$. In §4 we have seen that a vibration parallel to $O'A_1$ is propagated unchanged along the direction P′ in the convergent light figure. Hence the point P_a—representing the state of polarisation of one of the waves propagated in this direction—coincides with A_1. The state P_a being given, the state P_b may be immediately located as described in §5 *c*. Thus since the arc P_bY_k should be equal to arc A_1X_k *the state* P_b *must lie on the dotted small circle* of angular radius Y_kA_2 drawn about Y_k as centre. Further P_b and A_1 should lie on the same side of the great circle drawn through B, X_k and B′, and arc P_bB' should be equal to arc A_1B. From the symmetry of the figure, P_b is clearly determined by the point of intersection of the dotted small circle (mentioned above) with the arc Y_kP_b which is drawn at an angle 2θ to the equator as indicated, θ being the angle A_1X_kB. Turning to the convergent light figure (Fig. 1, text) suppose the point P′ on which we have fixed our attention moves outwards from the optic axis O_1 along the hyperbolic segment O_1A_1; the state of elliptic polarisation B (which would have been propagated along

the direction P′ as the slower wave *in the absence of absorption*) changes progressively from a left-circular vibration (for P′ coinciding with the optic axis O_1) towards the state of a linear vibration parallel to $O'A_1$: that is, on the Poincaré sphere (Fig. 2 *b*, text) the point B moves down from C_l towards A_1 along the arc C_lA_1, θ decreasing from $\frac{1}{2}\pi$ to zero. At the same time the state P_b of the faster wave being determined by the angle 2θ moves from A_2 towards A_1' along the dotted small circle whose diameter is A_2A_1' (the locus of P_b being in the lower hemisphere).

We shall now express the above results in physical terms. For all points on the hyperbolic segment O_1A_1 the state of polarisation P_a of the slower wave remains linearly polarised parallel to $O'A_1$ (§4). But as we proceed outwards from the optic axis O_1 along this hyperbolic segment, the state of polarisation P_b of the faster wave progressively alters in a manner which may be described thus: the state P_b—which is initially linearly polarised parallel to $O'A_2$—opens out into a right-elliptic vibration the ellipticity of which initially increases, the major axis at the same time turning rapidly towards the direction $O'A_1'$ orthogonal to $O'A_1$; further out the ellipticity again decreases though the turning of the major axis towards $O'A_1'$ continues, so that towards the border of the figure the states of the two waves approximate to those given in §5 *b*—and thence towards vibrations linearly polarised along the principal planes of linear birefringence (*see* Fig. 1, text).

As we proceed outwards from the optic axial direction O_1 along the hyperbolic segment O_1A_1', the state P_b of the faster vibration will, on the Poincaré sphere, remain fixed at A_1: but the state P_a of the slower vibration may be shown (by a similar analysis) to move from A_2 towards A_1' along the arc of a small circle which again has A_1A_2' as diameter, but which now lies in the *upper* hemisphere. So also, as we proceed along the hyperbolic branch $A_2O_1A_2'$ from A_2 to A_2', the state of polarisation of *one* of the waves will, according to §4, remain fixed at A_2 on the Poincaré sphere. (This state represents the slower state for points on the segment O_1A_2 but becomes the faster state for points on segment O_1A_2'). At the same time the state of the other wave moves on the Poincaré sphere from A_2' to A_1 and back to A_2' tracing (in a clockwise sense) the small circle of diameter $A_2'A_1$. (The results of this paragraph follow from those quoted at the end of §5*c*.) The variation of the states of polarisation of the waves for points on the hyperbolic branches $A_1O_1A_1'$ and $A_2O_1A_2'$ has been illustrated in Fig. 1, text.

According to a well-known property of the Poincaré sphere, the elliptic state P_b in Fig. 2 *b*, text, may be produced by passing a linear vibration in the state A_1' through a mica plate of retardation 2θ whose slow

vibration-direction is represented by X_k; *i.e.*, by passing light first through a polaroid whose vibration-direction is parallel to $O'A_1'$ and then through a retardation plate whose slow vibration is parallel to the axial plane. In Fig. 9 this arrangement was kept in front of the crystal plate, while behind the crystal plate was placed an 'elliptic analyser' which was kept automatically crossed with respect to the elliptic polariser (the arrangement used being that described in Part I, §5); it will be seen that, in conformity with theory, a particular point (such as P′) on the hyperbolic segment O_1A_1 is extinguished—this point representing the direction where the incident elliptic vibration is propagated unchanged. When the coupled retardation plates are rotated around together by 90° (so that X_k becomes the *fast* vibration-direction of the first retardation plate), a corresponding point on the hyperbolic segment O_1A_1' is extinguished—as seen in Fig. 10. In Figs. 11 and 12 (Plate XII) the coupled polaroids have been turned so that in both cases the vibration-direction of the first polaroid is parallel to $O'A_2'$ (represented by A_2' on the Poincaré sphere); the slow vibration-direction of the first retardation plate lies along the axial plane in Fig. 12 but perpendicular to it in Fig. 11. In the former case the point near O_1 which is extinguished lies on the hyperbolic segment O_1A_2, while in the latter (Fig. 11) it lies on O_1A_2'. In all the four photographs (Figs. 9–12, Plate XII) the extinguished points should lie on a curve of constant linear birefringence —a point which is difficult to confirm exactly. It was however verified that when the experiments were repeated with mica plates of lower retardation, the extinguished spots had in all cases moved outwards along the respective hyperbolic arcs. All these observations confirm the theoretical results stated in this section.

§7. SINGULAR AXES

We shall now consider directions of propagation for which the principal planes of linear birefringence are equally inclined to the axial plane. Considering first a point on the hyperbolic segment O_1M (Fig. 3 *b*, text), the orientation of the principal plane of linear birefringence OX_τ will be parallel to O′M, and will be represented by the point M on the Poincaré sphere (Fig. 4 *a*, text). Hence for this direction of propagation the state B (representing the slower wave in the absence of dichroism) will be a point on the meridian C_lM, at latitude $2\omega_1$; and the elliptic birefringence Δ in the absence of dichroism will [according to P–*a* Eq. (1)] be equal to $|2\rho|$ cosec $2\omega_1$. The great circle CX_kC' is drawn having B and B′ as its poles. The arc X_kB is a quadrant, and from the condition that the angle it subtends at P_a should be a right angle, it may be seen geometrically [or from P–*a*, Eq. (5)] that P_a

must lie either on the arc CX_k ($2\phi_a = \frac{1}{2}\pi$) or on the meridional arc BC ($2\psi_a = \frac{1}{2}\pi$). The former situation is illustrated in Fig. 4 *a*, text, and holds when the direction under consideration is still sufficiently close to the axial direction O_1 for k to be greater than Δ. It may be shown [using Eq. (1) above, and P-*a*, Eq. (4)] that the states P_a and P_b are the points of intersection of the great circular arc X_kCY_k with the small circle $E_2A_1E_1$ of spherical radius MA_1 drawn about M as centre. As we proceed outwards from the optic axis O_1 along the segment O_1M, Δ increases while at the same time the latitude $2\omega_1$ of the point B decreases: thus the states P_a and P_b which originally coincide with A_1 and A_2 move along the small circle towards the state E_1.

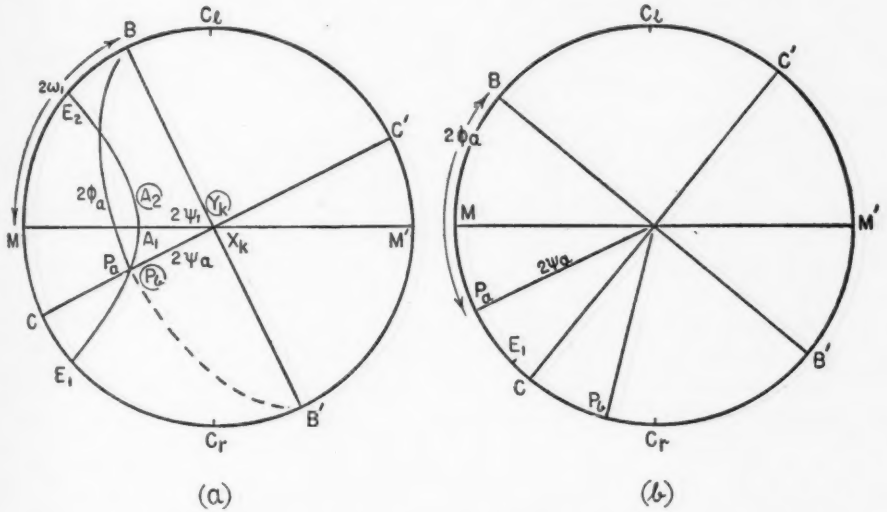

TEXT-FIG. 4. Construction for determining the states of polarisation of the propagated waves (*a*) for points on O_1S_1 in Fig. 3 *b*, text, (*b*) for points on S_1M in Fig. 3 *b*, text. The states E_1 and E_2 are respectively propagated unchanged along the singular axes S_1 and S_2.

In Fig. 3 *b*, text, S_1 denotes the direction of propagation on the segment O_1M for which Δ has become equal to k: since $\Delta = |2\rho| \operatorname{cosec} 2\omega_1$, it may be seen from Eq. (1) that for this direction $\omega_1 = \psi_1$ so that the point C of Fig. 4 *a*, text, now coincides with E_1. *For the direction of propagation S_1 there are no longer two distinct states of polarisation which can be propagated unchanged* since both states P_a and P_b have coalesced with the state represented by E_1 on the Poincaré sphere. Thus there is only *one* state of vibration which can be propagated without change of form along the '*singular*

axis' S_1—as may be directly shown from P–*a*, Eqns. (4) and (5) by setting $k = \Delta$, and $2\chi' = \frac{1}{2}\pi$. As we proceed further outwards along the segment O_1M, we will have $\Delta > k$; the states of polarisation P_a and P_b of the waves become again separate, moving from E_1 towards M and M′ respectively, along the arcs joining E_1 to these points. Thus Fig. 4 *b*, text, illustrates the position of the states P_a and P_b for a direction of propagation on the segment S_1M. The variation of the states of polarisation of the waves as we proceed outwards along O_1M' may be similarly traced on the Poincaré sphere using the relations stated in the concluding paragraph of §5 *c*. The direction S_2 for which $k = \Delta$, is again a singular axis where *only* the state of polarisation E_2 can be propagated unchanged—the points E_2 and E_1 being related to one another by reflection about the equatorial plane of the sphere.

The results proved above have been expressed in terms of the Poincaré sphere. They may be easily translated into physical terms, and the actual variation of the states of polarisation of the waves along the segments O_1M and O_1M' has been depicted (in an exaggerated form) in Fig. 3 *b*, text. The single wave which can be propagated along the singular axis S_1 differs from that which can be propagated along S_2, only in the sense of description; but both states are elliptically polarised and are not orthogonal to one another—unlike the case in inactive absorbing crystals.

Fig. 13 (Plate XIII) shows the photograph obtained with an elliptic polariser and a crossed elliptic analyser (*see* Part I, §5), the elliptic polariser being adjusted to produce the state of polarisation E_2 which can be propagated unchanged along the singular axis S_2; the vibration-direction of the first polaroid was kept along the direction $O'A_2$ (which is represented by the state A_2 in Fig. 4 *a*, text), this being followed by a quarter-wave plate with its slow axis along O′M (represented by M in Fig. 7). The singular axis S_2 and a corresponding singular axis associated with the other optic axis, appear extinguished in Fig. 13, Plate XIII. By turning the coupled polaroids so that the vibration-direction of the first polaroid is parallel to $O'A_1$ we observe the figure presented with an elliptic polariser E_1 and a crossed elliptic analyser. Fig. 14 shows this photograph, the singular axis S_1 and a corresponding singular axis associated with the optic axis O_2, being extinguished. (The singular axes have been indicated by spots in Figs. 13 and 14.) Fig. 15 shows the photograph obtained with the elliptic analyser removed in the arrangement of Fig. 14. This has to be compared with Fig. 16 which has been obtained by turning the polaroid by 90° relative to its orientation in Fig. 15. In Fig. 16, therefore, the elliptic vibration incident on the crystal is *orthogonal* to that which alone can be propagated unchanged along the singular axis S_1. Nevertheless, *the light incident along*

this singular direction is not reflected away; in fact the intensity of the light emerging along S_1 in Fig. 16, Plate XIII is *greater* than in Fig. 15, though in the latter case the incident vibration is in a state which is propagated unchanged along S_1. We need not enter into the explanation of this phenomenon, since it follows exactly along the lines given previously for a corresponding phenomenon observed in *inactive* absorbing crystals;[5, 6] the principle of superposition must be directly applied and the vibration incident along the singular direction S_1 in Fig. 16, Plate XIII will be propagated with a progressive change in its state of polarisation.

For any direction of propagation lying within the small strip $S_1O_1S_2$ (Fig. 3 *b*, text) the refractive indices of the waves will be equal according to P-*a*, Eq. (13), since for such a direction we have, $2\phi_a = \frac{1}{2}\pi$ from Fig. 4 *a*, text; the absorption coefficients of the waves will however be different according to P-*a*, Eq. (10), tending to equality only as the singular directions are approached. For the remaining points on the hyperbolic branch MO_1M', it is the refractive indices of the two waves which are different, the difference increasing from zero as we proceed outwards from the singular directions; while *the absorption coefficients are equal for this zone of directions* since $2\psi_a = \frac{1}{2}\pi$ from Fig. 4 *b*. Now in all the interference figures observed when the states of the polariser and analyser are crossed, the minima of the ring system should appear perfectly dark only along the zones where the absorption coefficients of the waves are equal [P–IV,[6] Eq. (21)]. Thus Figs. 1–6 and Figs. 9–14 confirm that the absorption coefficients of the waves are equal for points on the rectangular hyperbola one branch of which has been marked MO_1M' (the small strips joining the singular axes being excepted). This is also confirmed by the appearance of Brewster's brushes along the same zones—a feature which is to be theoretically expected from P–IV, Eq. (11) (following the same reasoning as for inactive absorbing crystals[7]), since the sum of the absorption coefficients of the waves may be taken to be constant over the region under consideration according to P-*a*, Eq. (9).

§8. Phenomena with Polariser alone and Analyser alone

In a previous publication[6] it has been explained quite generally that in crystals where the waves propagated along any direction are non-orthogonally polarised, interference rings should be exhibited with a polariser alone in front of the plate (*i.e.*, with no analyser); and also with an analyser alone behind the plate, the incident light being unpolarised. The ' idiophanic rings ' of the former class are exhibited in Figs. 17–20, for various settings of the linear polariser as the latter is turned in a clockwise sense—starting with the setting for which the vibration-direction is along the axial plane, as in

Fig. 17. Similarly, Figs. 21–24 show the idiophanic rings for various settings of a linear analyser as the latter is turned in an *anti*-clockwise sense, starting with the setting of Fig. 21, where the vibration-direction lies along the axial plane. In the observations with a polariser alone it was found that two hyperbolic brushes passing through the optic axes were formed in the setting of Fig. 18, Plate XIII, for which the vibration-direction of the polaroid was parallel to $O'A_2$ in Fig. 1, text; but Fig. 24 obtained with an analyser alone in the same setting is entirely different. So also in observations with an analyser alone, two hyperbolic brushes passing through the axial directions formed in the setting of Fig. 22, Plate XIV, where the vibration-direction of the polaroid was parallel to $O'A_1'$, in Fig. 1, text; but Fig. 20, obtained with a polariser alone in the same setting, is entirely different from Fig. 22.

Thus *the effects presented with a linear polariser alone are, in general, not the same as with a linear analyser alone* in the same setting. This proves that the non-orthogonally polarised states propagated along a general direction *cannot* be of the special type propagated in inactive absorbing crystals (*see* P–IV, §7).

It is physically understandable that the setting of the polaroid at which an optic axial direction, *e.g.*, O_1 appears darkest, differs according as whether the polaroid is set before or after the plate. In the former case the polariser-vibration would have to be parallel to $O'A_2$, *i.e.*, to the vibration-direction of the more heavily absorbed wave propagated along O_1; while in the latter case the analyser-vibration has to be parallel to $O'A_2'$ so that it will be *crossed* with respect to the vibration-direction of the *less* absorbed wave propagated along O_1. It remains to explain why at these settings, we find a whole zone of directions, represented by the hyperbolic brushes in Figs. 18 and 22, which appear as dark as the optic axial directions. For this purpose it must be remembered that the coefficients of linear dichroism as well as the orientations of the principal planes of linear dichroism are taken as constant over the region considered; so that the absorption coefficient of a wave propagated along any direction becomes purely a function of its state of polarisation: more precisely, *the absorption coefficient is purely a function of the angular distance* 2ϕ *of this state from* X_k, on the Poincaré sphere [P–*a*, Eq. (9)]. For the zone of directions of the rectangular hyperbola, one branch of which is marked $A_2O_1A_2'$ (Fig. 1, text), the state of polarisation of one of the waves is constant—being linearly polarised parallel to $O'A_2$ (§4). Hence when the vibration-direction of the polariser lies along $O'A_2$, the light suffers equal absorption all along this zone of directions, giving rise to hyperbolic brushes of uniform depth as in Fig. 18.

Similarly, consider any direction of propagation such as P′ on the rectangular hyperbola, one branch of which is $A_1O_1A_1'$. For any such direction the absorption coefficient of the more heavily absorbed wave will always be equal to the absorption coefficient (a_2 say) of the more heavily absorbed wave propagated along an optic axis such as O_1; this follows because according to §6, both these states (P_b and A_2) lie on a small circle with X_k as centre, and hence are at the same angular distance from X_k on the Poincaré sphere (Fig. 4 *a*, text). When unpolarised light of unit intensity is incident on a direction such as P′ the two non-orthogonally polarised waves (in states A_1 and P_b) into which it is split will both have initial intensities equal to $\frac{1}{2}\sec^2\frac{1}{2}A_1'P_b$ (*see* reference 8, §7). When a polaroid is kept behind the plate with its vibration-direction parallel to $O'A_1'$ it completely crosses out the less absorbed wave emerging along the direction P′ since this wave is linearly polarised parallel to $O'A_1$ (§4); a fraction $\cos^2\frac{1}{2}A_1'P_b$ of the intensity of the more heavily absorbed wave will however be transmitted by the analyser along the direction P′. Thus in the idiophanous figure observed with the analyser-vibration parallel to $O'A_1'$, the intensity of all points such as P′ (lying on the rectangular hyperbola, one branch of which is $A_1O_1A_1'$) will be equal to $\frac{1}{2}\exp(-a_2d)$, *i.e.*, it will be the same as the intensity of the axial direction in Fig. 18, Plate XIII. This explains the occurrence of the dark brushes in Fig. 22.

It has been shown in P–IV, §7, that the idiophanous figures presented with a polaroid set before or after the plate will not differ *if* the following condition is satisfied; on the Poincaré sphere, the angular distances of the points P_a and P_b (representing the states propagated along any direction) from the point representing the vibration-direction of the polaroid, should be supplements of one another. From the results of P–*a*, §4, it may be seen that this condition will be satisfied in the *particular* cases when the vibration-axis of the polaroid coincides with X_k or Y_k, *i.e.*, with one of the principal planes of linear dichroism $O'X_k$ or $O'Y_k$. This explains why Figs. 17 and 21 appear identical, as also Figs. 19 and 23.

It will be noted from the photographs that the idiophanous figures presented with a linear polariser at a setting of $+\theta$ to the axial plane is similar in some respects to that presented with a linear analyser at the setting $(-\theta)$ to the axial plane—the figures in the two cases being in fact related merely by reflection about the vertical line Y_kY_k' (*Compare* Fig. 18 with Fig. 22, and Fig. 20 with Fig. 24). This may be explained using the results stated at the end of §5 *c*; the intensity at the point $P(\delta, \chi)$ with the polariser-vibration at $+\theta$ to $O'X_k$ [being given by P–IV, Eq. (6)] may be shown

to be equal to the intensity at P (δ, $-\chi$) with the analyser-vibration at ($-\theta$) to $O'X_k$ [as obtained from P–IV, Eq. (16)].

Finally it may be mentioned that observations with a polariser alone and with an analyser alone readily revealed a characteristic difference in the behaviour of a *left*-rotating sector (occurring in another basal plate). The orientations of the polaroid at which the brush formed in the two cases showed that the azimuth of the linearly polarised states propagated along the optic axes lay in the *positive* quadrant—as is to be expected from theory (P–*a*, §8 *b*).

The author is highly indebted to Prof. Sir C. V. Raman, for his unfailing interest in the present work.

SUMMARY

Using a wavelength (λ 5890) for which the linear dichroism of the amethystine sector is appreciable ($k > |2\rho|$), twenty-four interference figures are reproduced confirming in detail the theory of light propagation in absorbing crystals possessing optical activity.[1] Unlike the behaviour in transparent crystals, the idiophanic interference figures seen with a polariser alone in front of the plate differ in general from those presented with an analyser alone behind the plate in the same setting. The existence of four singular axes, one on either side of each optic axis, is shown: along each singular axis only *one* (elliptically) polarised wave—and not two—can be propagated without change of form.

REFERENCES

1. Pancharatnam, (P–*a*) .. *Proc. Ind. Acad. Sci.*, 1957, **46 A**, 280.
2. ———— .. *Ibid.*, 1956, **44 A**, 247.
3. Johannsen .. *Manual of Petrographic Methods*, McGraw-Hill, 1918, 440.
4. Wooster .. *A Text-book on Crystal Physics*, Cambridge, 1938, 141.
5. Pancharatnam .. *Proc. Ind. Acad. Sci.*, 1957, **46 A**, 86, 235.
6. ————, (P–IV) .. *Ibid.*, 1957, **45 A**, 2.
7. Pockels .. *Lehrbuch der Kristalloptik, Teubner*, 1906, 421.
8. Pancharatnam .. *Proc. Ind. Acad. Sci.*, 1956, **44 A**, 398.
9. ———— .. *Ibid.*, 1954, **40 A**, 196.
10. Dove .. *Farbenlehre*, 1853, Seite 251.
11. Liebisch .. *Ber. Berl. Akad.*, 1916, **36**, 870.
12. Leitz and Munchberg .. *Neues Jb. Mineral*, 1956, **10**, 217.

APPENDIX

It was shown in a previous investigation[9] on amethystine quartz that the approximate orientation of the absorption ellipsoid could be derived purely from observations on the pleochroism made at appreciable inclinations to the *c*-axis. As regards the observations in convergent light and their explanation described in that paper, they have no doubt to be supplemented by the account given in the present paper—but this does not alter the conclusions already drawn from them. Thus the present paper establishes rigorously that if we consider the section of the absorption ellipsoid normal to the *c*-axis, then the major semi-axis of the elliptic section coincides with the obtuse-bisectrix—*which in turn coincides with an* a-*axis of quartz*. The method, previously used, of determining the orientations of these principal axes for less intensely coloured areas by observations with a single polaroid* may also be rigorously justified using the results stated at the end of §8. Very significant too is the fact that the intensity of Brewster's brushes (Part I, Fig. 5, Plate IX) appears symmetrical about the plane $Y_kY_{k'}$ but not about the axial plane. This indicates that the plane $Y_kY_{k'}$ (normal to the *a*-axis mentioned) is a plane of symmetry of the absorption ellipsoid—though this is not true of the axial plane. This is confirmed by the appearance of Brewster's brushes in white light: the two brushes below the axial plane appear bluish purple towards the border of the figure while those above are of a deeper reddish purple colour. The explanation of this is that there are two colour axes in the symmetry plane $Y_kY_{k'}$ which lie on either side of the *c*-axis at approximately 45° to it—the colours for vibrations along these axes being blue and deep red respectively.

According to the results of our previous investigation[9] the amethystine material occurring in the quartz can take up one of several discrete optic orientations all consistent with the description given above. An overlap of amethystine material of different optic orientations can be produced by one or more of the following three factors: (1) overlap of sectors associated with different rhombohedral faces, (2) optical twinning in which the different twin members are of opposite handedness, (3) electrical twinning in which the electrical axes of the different twin members are in opposite orientation. The main difficulty of studying the pleochroism of amethyst in any random section plate is that optical twinning of an interpenetrant variety occurs

---

* Brewster's brushes had been referred to in our earlier paper[9] as the idiophanous figure —a term reserved in the present paper for the figure presented with a polariser or analyser alone in conformity with the more prevalent usage.

extensively. Some of the investigations of Dove[10] and Liebisch[11] are of value in interpreting the interference figures in such optically twinned areas, but they do not directly concern the investigations presented in this paper.

Subsequent to our previous publication on the pleochroism of amethyst there has appeared an interesting paper by Lietz and Munchberg[12] dealing with the same problem. The difference between their conclusions and ours certainly appears to raise the interesting possibility of the existence of different species of amethyst with entirely different optical chracteristics.† Nevertheless, it would be difficult to decide how far there is real disagreement between our conclusions and the experimental part of their observations. The existence of pleochroism along the *c*-axis is common ground: and because the subject of refractive index and absorption are closely interlinked by dispersion theory, it follows that the index ellipsoid could not be strictly uniaxial for all wavelengths. In view of this fact their statement that amethyst possesses uniaxial symmetry can only be taken to mean that the index ellipsoid is *very nearly* uniaxial. With this we are in complete agreement, if we restrict ourselves to sectors of moderate colouration such as they have chosen. The mean absorption coefficient of the sector which was used by them for observing the interference figure was about $0{\cdot}75\ \text{cm.}^{-1}$ for wavelengths near the absorption maximum; whereas for the sector used in the present investigation the *difference* k between the absorption coefficients for vibrations parallel to $O'Y_k$ and $O'X_k$ is itself about 15 times that value (*see* §3). Using the same sector as employed in the present investigation the absorption spectrograms for vibrations along the three colour axes had been reproduced in our previous paper: though the actual wavelengths of the absorption maxima were only qualitatively located, the spectrograms clearly showed the difference in intensity and position of the absorption maxima, especially for the two main absorption axes (red and blue). The latter difference would not have been present if there had been electrical twinning. Also—considering the great breadth of the absorption band in amethyst—we do not know whether the shift of the absorption maxima could have been easily detected if the sector had not been so intensely coloured, and if the vibrations had not been polarised exactly along the colour axes. Regarding this point, however (*viz.*, the orientation of the principal axes of the absorption ellipsoid), the conclusions of Leitz and Munchberg differ from ours. This would again appear to point more clearly to a fundamental difference in the nature of the amethystine material investigated in

† The material studied by us were mainly from Hyderabad, but included a few uncut specimens from Uruguay.

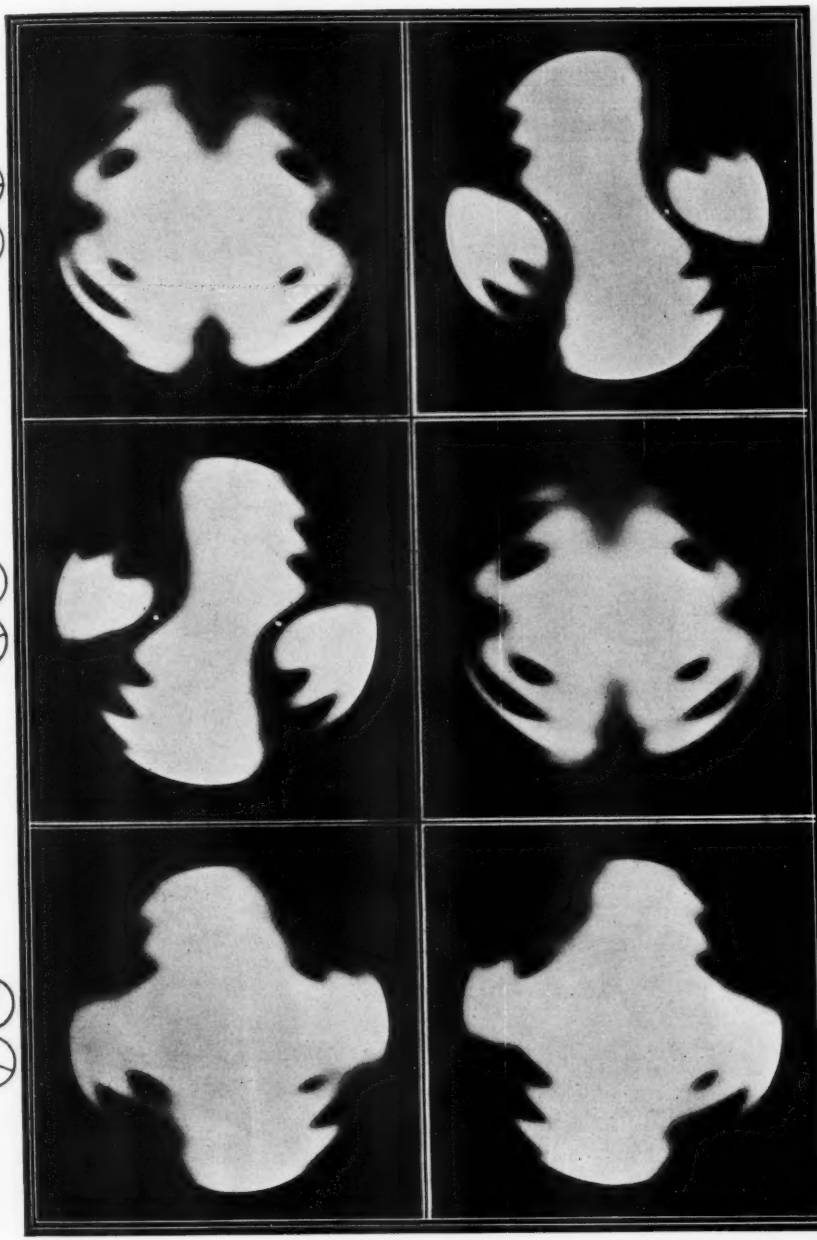

FIG. 1 FIG. 2

FIG. 3 FIG. 4

FIG. 5 FIG. 6

FIGS. 1–6

Interference Figures observed between crossed polaroids.

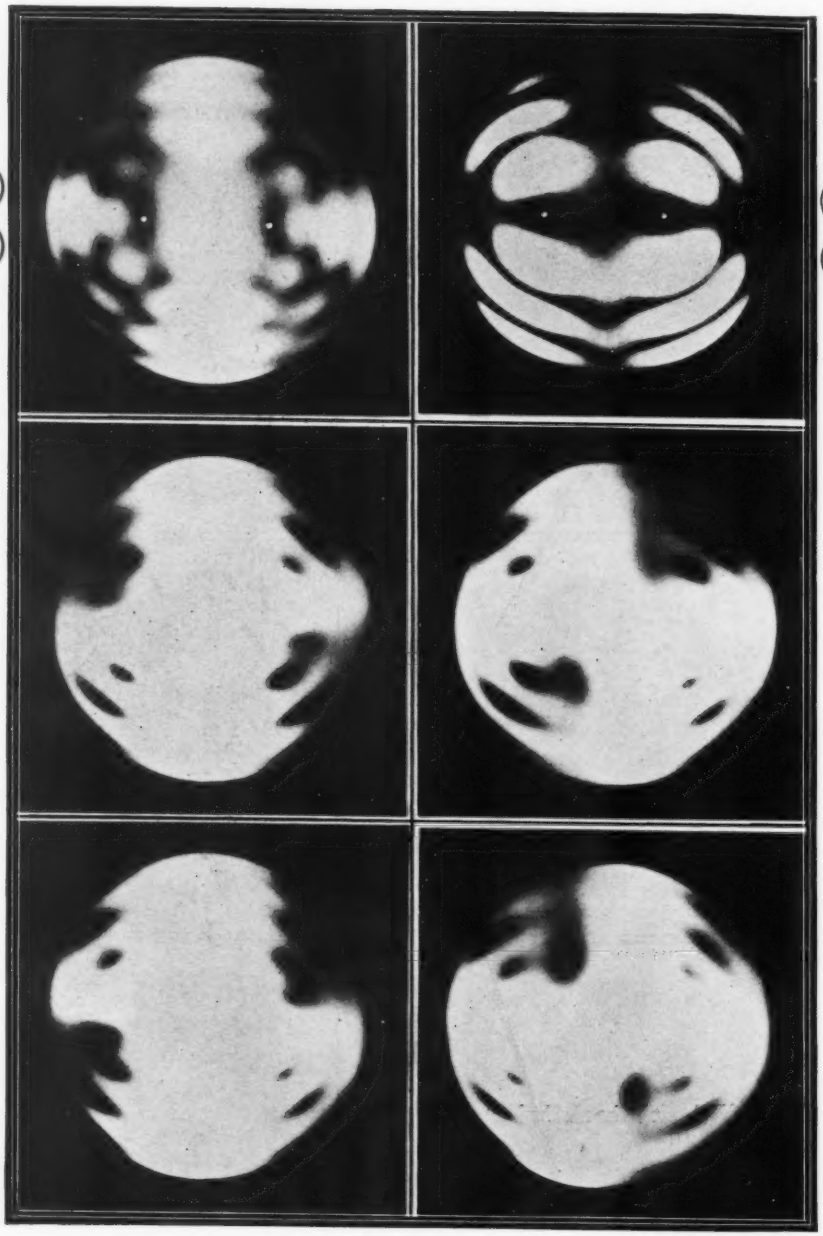

FIG. 7 FIG. 8

FIG. 9 FIG. 10

FIG. 11 FIG. 12

FIGS. 7–12

FIG. 8

FIG. 10

FIG. 12

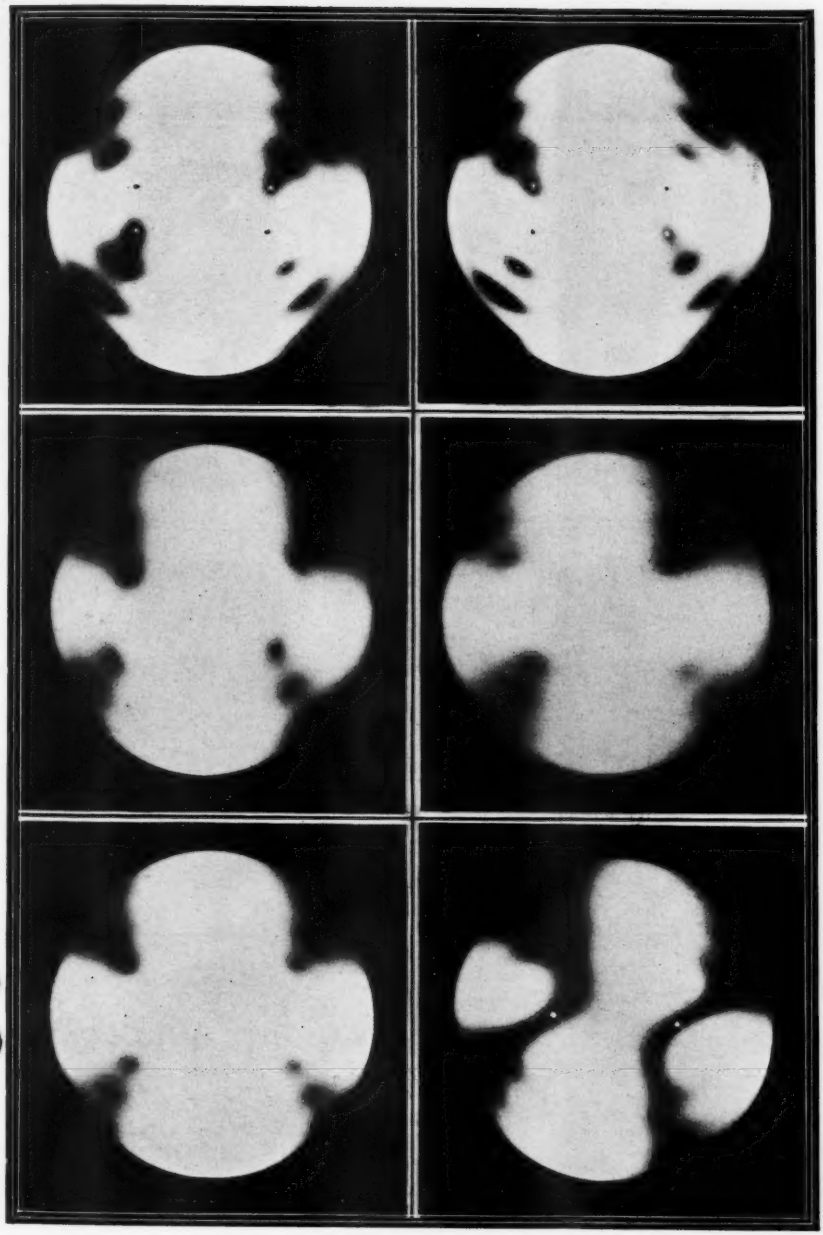

FIG. 13

FIG. 14

FIG. 15

FIG. 16

FIG. 17

FIG. 18

FIGS. 13-18

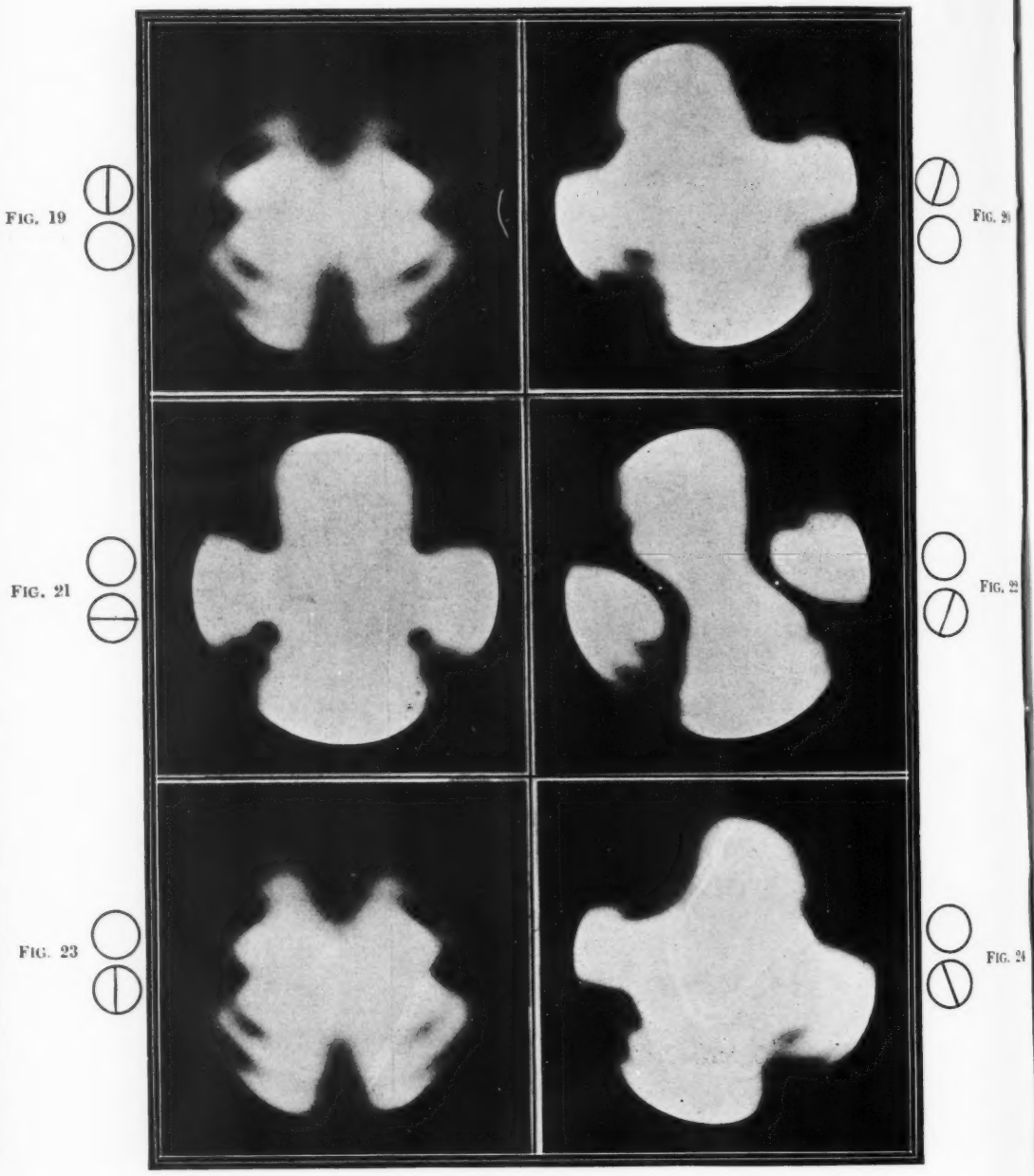

FIGS. 19–24

Phenomena with polariser alone, and analyser alone.

the two cases. But before this can be asserted with any confidence the following fact must also be taken into account: that for finding the orientation of the principal axes of the absorption ellipsoid it is *not* sufficient to measure the absorption for three mutually perpendicular vibrations. This has been done by Leitz and Munchberg by observations through the faces $(10\bar{1}0)$ and $(1\bar{2}10)$. (The observations through the basal section are of course only useful for showing the absence of uniaxial symmetry, unless account is taken theoretically of the presence of optical activity.)

THE FACTORS THAT AFFECT ALKALI COLOUR REACTIONS OF FLAVONOLS: A STUDY OF FLAVONOLS OF UNCOMMON TYPES

By V. K. Ahluwalia, N. R. Krishnaswami, S. K. Mukerjee
V. V. S. Murti, T. R. Seshadri, F.A.Sc., and C. Venkataramani
(*From the Department of Chemistry, Delhi University, Delhi*)

Received January 13, 1958

In a number of earlier papers it has been pointed out that colour changes in alkaline buffer solutions can serve as useful indications of the constitution of flavonoids. Flavonols of the gossypetin series having the 5: 7: 8-arrangement of hydroxyl groups in the condensed benzene ring exhibit prominent colours and also a display of colours.[1] This is more marked in the case of flavonols of the calycopterin series having the 5: 6: 7: 8-tetrahydroxy benzene ring.[2] Both these groups of compounds also undergo ready conversion into quinones when treated with *p*-benzoquinone. Somewhat similar properties though less marked are possessed by myricetin[3] and robinetin,[4] 6-hydroxy myricetin[5] and 6-hydroxy robinetin[6] in which the side phenyl nucleus carries three hydroxyls in the 3′, 4′ and 5′ positions. Since the corresponding flavones do not show such prominent colours, the hydroxyl in the 3-position, characteristic of flavonols, seems to be an essential requisite.

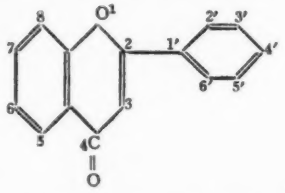

The quercetagetin series of flavonols in which the 5: 6: 7-arrangement of contiguous hydroxyl groups is present do not give prominent alkali colour reactions except the highest member having the 3′: 4′: 5′-hydroxy groups.[5] In the case of nor-gardenin[7] (3: 5: 6: 8: 3′: 4′: 5′- heptahydroxy flavone) the colour reaction is again not prominent and there is no display of colours though in the condensed benzene nucleus of this flavonol there is a hydroxy quinol system involving the 5: 6: 8-positions and the side phenyl nucleus has three hydroxyl groups as in robinetin. It appeared therefore that more factors are involved than known before; probably it was essential to have

a hydroxyl free in the 7-position and the exact distribution of the hydroxyl groups was an important consideration. In order to throw more light on these questions, a number of new flavonols have been prepared and studied during the past several years and the results are collected in this paper.

A few flavonols without a 7-hydroxyl group but otherwise having favourable structures have now been examined. They were prepared from some of the intermediates in the synthesis of gardenin[10] and they are 3:5:3′:4′:5′-pentahydroxy flavone and 3:5:8:3′:4′:5′-hexahydroxy flavone. Though they do not give as deeply coloured solutions as the corresponding flavonols having the 7-hydroxyl group, they are somewhat better than nor-gardenin. Hence it would appear that the 5:6:8-arrangement of hydroxyl groups is a disadvantage.

As already mentioned prominent colours are exhibited by myricetin and robinetin which have the three hydroxyl groups in the side phenyl nucleus in the 3′:4′:5′-positions. In an earlier paper[6] flavonols having a quinol-system in the side phenyl nucleus, *i.e.*, 2′:5′-dihydroxy compounds were reported and were shown to exhibit very feeble alkali colour changes as compared with the 5:8-dihydroxy compounds, *e.g.*, 3-hydroxy primetin,[9] though both were quinols. To study further the part played by the side phenyl nucleus in alkali colour reactions, 3:5:7:2′:3′:4′-hexahydroxy and 3:7:2′:3′:4′-pentahydroxy flavones have now been synthesised. As compared with myricetin and robinetin, they give feeble alkali colour reactions and lack colour display. The isomers of quercetin and fisetin having 2′:3′-dihydroxy groups have also been prepared and compared with quercetin and fisetin. The 2′:3′-combination reduces appreciably the intensity of colour reactions.

Fluorescence in alcohol and particularly in sulphuric acid solutions appears to be of good diagnostic value. A characteristic feature of fisetin, quercetin, robinetin and myricetin is their marked capacity to exhibit fluorescence in concentrated sulphuric acid solutions while their methyl ethers show only diminished fluorescence. This is markedly absent in the isomeric compounds and their methyl ethers reported in this paper.

Experimental

(All compounds were dried in vacuo at 110° C. over phosphorus pentoxide before analysis.)

3:5:3′:4′:5′-*Pentahydroxy flavone*.—5-Hydroxy-3:3′:4′:5′-tetramethoxy flavone[10] (0·5 g.) was demethylated by refluxing with a mixture of acetic anhydride (15 c.c.) and hydriodic acid (10 c.c.) for 1·5 hrs. The

product (0·2 g.), yellow prisms from a mixture of ethyl acetate and petroleum ether, melted at 278–80° with earlier darkening at 272° (Found: C, 59·7; H, 3·9; $C_{15}H_{10}O_7$ requires C, 59·6; H, 3·3%). It gave a green colour with alcoholic ferric chloride and dissolved very slowly in aqueous sodium bicarbonate (5%) giving an orange yellow solution. Its pale green solution in aqueous sodium carbonate (5%) quickly changed to purple red and then slowly to brown. In aqueous sodium hydroxide (5%) it showed a transient green colour changing to purple which on shaking rapidly became brown.

The penta acetate, colourless rectangular plates from ethanol, melted at 207–8°.

3:5:3′:4′:5′-*Pentamethoxy flavone.*—Methylation of the above 5-hydroxy flavone (0·5 g.) with dimethyl sulphate (1 c.c., excess) and potassium carbonate (2 g.) in acetone for 30 hrs. yielded the pentamethyl ether (0·4 g.). It came out of ethyl acetate as thin rectangular plates, m.p. 152–53° (Found: C, 64·8; H, 5·2; $C_{20}H_{19}O_7$ requires C, 64·7; H, 5·1%).

3:5:8:3′:4′:5′-*Hexahydroxy flavone.*—Obtained by the demethylation of 5:8-dihydroxy-3:3′:4′:5′-tetramethoxy flavone[10] (0·5 g.) with a mixture of hydriodic acid (10 c.c.) and acetic anhydride (15 c.c.), the hexahydroxy flavone crystallised from a mixture of ethyl acetate and petroleum ether as thick yellow prisms, m.p. 297–300° (Found: C, 56·0; H, 3·5; $C_{15}H_{10}O_8$ requires C, 56·6; H, 3·2%). It gave a green colour with alcoholic ferric chloride deepening with excess of the reagent. With aqueous sodium bicarbonate (5%) it gave a yellow colour. Its yellow solution in aqueous sodium carbonate (5%) changed to brown and finally to deep red. Its deep red solution in aqueous sodium hydroxide (5%) changed to dark brown.

The hexa acetoxy flavone crystallised from ethyl acetate as colourless, small rectangular plates melting at 236–37°.

3:5:8:3′:4′:5′-*Hexamethoxy flavone.*—5:8-Dihydroxy-3:3′:4′:5′-tetramethoxy flavone[10] (0·3 g.) was completely methylated by dimethyl sulphate (1 c.c.) and potassium carbonate (3 g.) in acetone when refluxed for 30 hrs. It crystallised from a mixture of ethyl acetate and petroleum ether as colourless, thin plates melting at 170–71° (Found: C, 62·7; H, 5·5; $C_{21}H_{22}O_8$ requires C, 62·7; H, 5·5%).

o-Veratric anhydride.—A mixture of *o*-veratric acid[11] (20 g.), anhydrous ether (200 c.c.) and dry pyridine (20 c.c.) was well cooled in ice and salt mixture and treated with thionyl chloride (5 c.c.) in small quantities with good mixing. After keeping overnight in the refrigerator the anhydride was isolated by

the usual method. Colourless needles (16 g.) from petroleum ether, m.p. 93°. Heilbron[12] gives the same melting point.

7-*Hydroxy*-3:2′:3′-*trimethoxy flavone*.—An intimate mixture of ω-methoxy resacetophenone (3 g.), *o*-veratric anhydride (16 g.) and sodium *o*-veratrate (6 g.) was heated at 180-90° under reduced pressure for 6 hrs. and the product was worked up by the general procedure of Allan-Robinson condensations. Pale yellow, thick prisms from methanol (1·2 g.), m.p. 210–11° (Found: C, 66·2; H, 4·9; $C_{18}H_{16}O_6$ requires C, 66·7; H, 4·9%). It gave no colour with alcohoic ferric chloride. Its solution in concentrated sulphuric acid was yellow with no fluorescence. The acetatee (acetic anhydride-sulphuric acid method) crystallised as colourless, small prisms from ethyl acetate-petroleum ether, m.p. 125–26°.

Methylation with dimethyl sulphate and potassium carbonate in dry acetone medium gave 3:7:2′:3′-tetramethoxy flavone, colourless prisms from benzene-petroleum ether, m.p. 82–83° (Found: C, 66·4; H, 4·9; $C_{19}H_{18}O_6$ requires C, 66·7; H, 5·3%). Its solution in strong sulphuric acid was yellow and showed no fluorescence. Fisetin tetramethyl ether gave a yellow solution in concentrated sulphuric acid showing feeble green fluorescence.

3:7:2′:3′-*Tetrahydroxy flavone*.—Demethylation of the 7-hydroxy-3:2′:3′-trimethoxy flavone (0·3 g.) by refluxing for 2 hrs. in acetic anhydride (5 c.c.) with hydriodic acid (5 c.c.; d., 1·7) gave the tetrahydroxy flavone (0·15 g.), yellow prisms from ethyl acetate-benzene, m.p. 290–2° (decomp.) (Found: C, 62·8; H, 3·7; $C_{15}H_{10}O_6$ requires C, 62·9; H, 3·5%).

It gives a reddish-brown ferric reaction turning brownish-green with more reagent. In dilute sodium carbonate it dissolves to a bright yellow solution unchanged on keeping; fisetin gives a deep yellow solution turning brown gradually. With strong sulphuric acid it gives a pale yellow solution without fluorescence whereas fisetin yields a yellow solution showing bluish-green fluorescence.

The tetra-acetate was prepared with acetic anhydride and two drops of concentrated sulphuric acid; colourless long, thin plates from methyl alcohol, m.p. 204–5°.

5:7-*Dihydroxy*-3:2′:3′-*Trimethoxy flavone*.—A mixture of ω-methoxy phloracetophenone (4 g.), *o*-veratric anhydride (28 g.) and sodium *o*-veratrate (10 g.) was heated under reduced pressure at 170–80° for 7 hrs. The product (1·3 g.) crystallised from methanol as clusters of long, thin needles and tapering plates, m.p. 196–97° (Found: C, 62·3; H, 5·2; $C_{18}H_{16}O_7$ requires

C, 62·8; H, 4·7%). The substance gave a greenish-brown colour with alcoholic ferric chloride; its solution in concentrated sulphuric acid was yellow without any fluorescence. The diacetate crystallised from ethyl acetate and petroleum ether as colourless prisms, m.p. 118–19°.

Methylation by the dimethyl sulphate-potassium carbonate method gave 3:5:7:2′:3′-pentamethoxy flavone, colourless, thick rhombs (ethyl acetate-petroleum ether), m.p. 170–1°, giving a yellow solution in strong sulphuric acid without fluorescence (Found: C, 64·5; H, 5·7; $C_{20}H_{20}O_7$ requires C, 64·5; H, 5·4%). Quercetin pentamethyl ether dissolved in concentrated sulphuric acid to a yellow solution having feeble green fluorescence.

3:5:7:2′:3′-*Pentahydroxy flavone.*—The above dihydroxy flavone was demethylated by refluxing with acetic anhydride and hydriodic acid for 2 hrs. The product crystallised from alcohol as yellow, small prisms, m.p. 300° (decomp.) (Found: C, 59·1; H, 3·7; $C_{15}H_{10}O_7$ requires C, 59·6; H, 3·3%). It gives a greenish-brown ferric chloride colour. In concentrated sulphuric acid it forms a yellow solution without fluorescence while quercetin gives a yellow solution showing bluish-green fluorescence.

2:3:4-*Trimethoxy benzoic acid.*—No convenient preparative method for this compound seems to have been described before.

Method I.—Dry pyrogallol carboxylic acid[13] (50 g.) was dissolved in dry acetone (500 c.c.) and the solution was refluxed with dimethyl sulphate (140 c.c.) and potassium carbonate (200 g.) for 40 hrs. The product isolated as usual, was taken up in ether and washed with aqueous alkali to remove any phenolic material; removal of the solvent gave the methyl 2:3:4-trimethoxy benzoate as an oil. This was refluxed with aqueous sodium hydroxide (10%; 200 c.c.), the alkaline solution extracted with ether and acidified yielding the 2:3:4-trimethoxy benzoic acid (30 g.), colourless needles (from hot water), m.p. 99°.

Method II.—Gallacetophenone[14] (50 g.) was completely methylated by refluxing with dimethyl sulphate (100 c.c.) and potassium carbonate (200 g.) for 40 hrs. The product was dissolved in ether and the ethereal solution freed from phenolic impurities by washing with dilute alkali. Evaporation of the solvent gave the trimethoxy acetophenone (62 g.) as a reddish oil. It was directly employed for the next stage.

To gallacetophenone trimethyl ether (30 g.) was added alkaline hypochlorite solution (250 c.c.; prepared by passing chlorine from 25 g. of potassium permanganate and 40 c.c. of concentrated hypochloric acid into

10% sodium hydroxide solution) in small quantities with vigorous shaking; the mixture was maintained at 60–75°, during this addition and for a further period of 3 hrs. It was cooled and the unoxidised ketone removed by extraction with ether. Acidification of the alkaline solution gave the 2: 3 : 4-trimethoxy benzoic acid as a colourless solid. The recovered ketone was again oxidised; total yield, quantitative. This sample was purer than that prepared by the first method.

2: 3: 4-*Trimethoxy benzoic anhydride.*—A mixture of 2: 3: 4-trimethoxy benzoic acid (30 g.), dry ether (200 c.c.) and dry pyridine (30 c.c.) was cooled in freezing mixture and treated with thionyl chloride (8 c.c.) in small lots with good mixing. After keeping overnight the anhydride was worked up. Crystallisation from benzene-petroleum ether gave colourless, thick prisms (26 g.), m.p. 86° (Found: C, 59·3; H, 5·6; $C_{20}H_{22}O_9$ requires C, 59·1; H, 5·4%).

7-*Hydroxy*-3: 2′: 3′: 4′-*Tetramethoxy flavone.*—A mixture of ω-methoxy resacetophenone (3 g.), 2: 3: 4-trimethoxy benzoic anhydride (26 g.) and the sodium salt of 2: 3: 4-trimethoxy benzoic acid (10 g.) was fused under reduced pressure at 170–80° for 6 hrs. and the product worked up as in similar cases. The flavone (0·8 g.) formed almost colourless prisms from methanol, m.p. 226–27° (Found: C, 64·1; H, 5·0; $C_{19}H_{18}O_7$ requires C, 63·7; H, 5·0%). It did not give any colour with alcoholic ferric chloride; its solution in concentrated sulphuric acid was yellow without any fluorescence. The acetate crystallised as long, thin needles and plates from ethyl acetate-petroleum ether, m.p. 120–21°.

3: 7: 2′: 3′: 4′-*Pentamethoxy flavone* was prepared by methylation of the 7-hydroxy compound with methyl sulphate and potassium carbonate in acetone solution; colourless, thick prisms from methanol, m.p. 145–46° (Found: C, 64·2; H, 5·3; $C_{20}H_{20}O_7$ requires C, 64·6; H, 5·4%). Its yellow solution in concentrated sulphuric acid did not have any fluorescence. Robinetin pentamethyl ether gave a yellow solution with a green fluorescence.

3: 7: 2′: 3′: 4′-*Pentahydroxy flavone.*—The above 7-hydroxy compound was demethylated with acetic anhydride-hydriodic acid and the product crystallised from ethyl acetate. Yellow, small prisms, decomposing at 314–15° (Found: C, 59·5; H, 3·6; $C_{15}H_{10}O_7$ requires C, 59·6; H, 3·3%). The following are the more important colour reactions shown by this compound:

Aqueous sodium carbonate (5%).—Deep yellow solution. On shaking with air turns orange red and then brown which fades off. Under these

conditions robinetin forms a blue solution changing to green, purple, brown which fades gradually.

Aqueous sodium hydroxide (2%).—Brown-red solution turning orange and finally pale brown. Robinetin gives a blue solution becoming green which changes to brown.

Alcoholic ferric chloride.—Greenish-brown, becomes bluish-green with more of the reagent and changes to violet on standing. With robinetin a greenish-brown colour develops turning brown with more of the reagent.

Concentrated sulphuric acid.—Yellow solution without fluorescence while robinetin dissolves to a yellow solution with green fluorescence.

The penta-acetate crystallised as colourless plates from ethyl acetate-petroleum ether, m.p. 185–86°.

5: 7-*Dihydroxy*-3: 2′: 3′: 4′-*Tetramethoxy flavone.*—A mixture of ω-methoxy phloracetophenone (3 g.), 2: 3: 4-trimethoxy benzoic anhydride (28 g.) and sodium salt of 2: 3: 4-trimethoxy benzoic acid (10 g.) was heated at 180–90° for 6 hrs. under reduced pressure and the product worked up as in the previous cases; the crude flavone was purified by chromatography over alumina in benzene solution and elution with benzene-acetone (1: 1) mixture. Pale yellow, thick prisms from alcohol (1·1 g.), m.p. 174–75° (Found: C, 61·3; H, 5·4; $C_{19}H_{18}O_8$ requires C, 61·0; H, 4·8%). It gave an olive-brown ferric reaction and a yellow solution in strong sulphuric acid without fluorescence. The diacetate (acetic anhydride and a drop of sulphuric acid) formed colourless prisms from ethyl acetate-petroleum ether, m.p. 146–47°.

The dihydroxy flavone was completely methylated by the methyl sulphate-potassium carbonate method giving 3: 5: 7: 2′: 3′: 4′-hexamethoxy flavone as colourless, small prisms from alcohol, m.p. 153–54° (Found: C, 62·4; H, 5·6; $C_{21}H_{22}O_8$ requires C, 62·7; H, 5·5%). It dissolved to a yellow solution in strong sulphuric acid without any fluorescence. Myricetin hexamethyl ether gave a yellow solution with green fluorescence.

3: 5: 7: 2′: 3′: 4′-*Hexahydroxy flavone.*—Demethylation of the above dihydroxy compound by the acetic anhydride-hydriodic acid method gave the hexahydroxy flavone as brownish-yellow prisms from methanol, decomposing at 308–10° (Found: C, 56·8; H, 3·4; $C_{15}H_{10}O_8$ requires C, 56·6; H, 3·2%). It showed the following colour reactions:

Aqueous sodium carbonate (5%).—Yellow solution becoming brown. Myricetin gives a deep green solution turning violet-brown, purple, red, orange and brown.

Aqueous sodium hydroxide (2%).—Yellow solution turning orange red. Myricetin dissolves to a green solution becoming blue and then brown.

Alcoholic ferric chloride.—Olive-green solution which turns brown on keeping. With myricetin an olive-green colour is obtained which becomes brown with more of the reagent. On standing the solution turns blue and a blue-black precipitate settles down.

Concentrated sulphuric acid.—Yellow solution without fluorescence while myricetin gives a yellow solution with bluish-green fluorescence.

Summary

In order to get fuller information on the influence of hydroxyl groups on alkali colour reactions a number of flavonols of types uncommon in Nature have been prepared and examined. Though the correlation between structure and alkali colour reactions is complex, when applied with care the reactions can be used for diagnostic purposes. The alkali colour reactions of the flavonols with 2′ : 3′ and 2′ : 3′ : 4′ disposition of hydroxyl groups are not prominent and their fluorescence properties are also very feeble.

References

1. Perkin .. *J.C.S.*, 1899, **75**, 825.
   Seshadri and co-workers .. *Proc. Ind. Acad. Sci.*, 1945, **22 A**, 157 and earlier papers.
2. Seshadri and Venkateswarlu .. *Ibid.*, 1946, **23 A**, 192.
3. Perkin .. *J.C.S.*, 1896, **69**, 1287.
4. Rajagopalan, Rangaswami, Rao and Seshadri *Proc. Ind. Acad. Sci.*, 1946, **23 A**, 62.
5. Row and Seshadri .. *Ibid.*, 1946, **23 A**, 35.
6. Rao, Rao and Seshadri .. *Ibid.*, 1945, **22 A**, 297.
7. Balakrishna and Seshadri .. *Ibid.*, 1948, **27 A**, 91.
8. Sehgal and Seshadri .. *Ibid.*, 1952, **36 A**, 355.
9. Seshadri, Varadarajan and Venkateswarlu *Ibid.*, 1950, **32 A**, 250.
10. Ahluwalia, Mukerjee and Seshadri .. *J.C.S.*, 1954, 3988.
11. Edwards, Perkin and Stoyle .. *Ibid.*, 1925, 195.
12. Heilbron .. *Dictionary of Organic Compounds*, 1953 Ed., p. 269.
13. Critchlow, Haworth and Pauson .. *J.C.S.*, 1951, 1323.
14. Badhwar and Venkataraman .. *Organic Syntheses*, 1934, **14**, 40.

GRAVIMETRIC DETERMINATION OF THORIUM AND ITS SEPARATION FROM URANIUM, CERITE EARTHS AND CERIC SALTS

By G. M. Saxena and T. R. Seshadri, F.A.Sc.

(Department of Chemistry, University of Delhi, Delhi-8)

Received June 8, 1957

Thorium has been an important element in the past, particularly in connection with the incandescent mantle industry and it has recently acquired added interest as a source of atomic energy. Hence its determination in its ores and also its separation from accompanying elements has become increasingly important. From a review of the methods of the determination of thorium, Kaufmann[1] and Wenger and Duckert[2] reported that some of the most sensitive reagents precipitate uranium and cerite earths along with thorium. Among those that have been subsequently considered to be effective for separating thorium from rare earths,[3–11] probably the most important are *m*-nitro-benzoic acid and tetrachlorophthalic acid. But even these suffer from interference by ceric ions and hence further processes have to be adopted. Another combination which is frequently found in nature is thorium and uranium. Several organic acids have been reported to be suitable for determining thorium in the presence of uranium: they are ferron,[12] *m*-nitro-benzoic acid,[13] anisic acid,[14] cinnamic acid,[15] benzoic acid[16] and sebacic acid.[17] But they are not useful in the presence of cerite earths or ceric salts and hence have not got into common use.

As the result of a detailed study of flavone and xanthone derivatives as complexing agents for rare metals,[17a] 1-hydroxy-3-methoxy xanthone has now been found to be a useful reagent for the determination of thorium in the presence of uranium (uranyl ion) and of cerite earths and ceric salts. When an alcoholic solution of this xanthone is added to thorium salt solution, a deep yellow solution is formed which on dilution with water gives a yellow precipitate yielding thorium dioxide on ignition.

Owing to the solubility of the thorium complex in organic solvents, it is not possible to separate the pure complex from the excess of the xanthone added. Hence its composition could not be determined by direct weighing. The spectrophotometric method of Job[18] and Vosburgh and Cooper,[19] however, shows that the complex has the molar composition ThL_4 where L represents the xanthone ligand. The estimation of thorium can be conveniently

done in the pH range 2·6–3·2 and under these conditions a minimum limit of 10·0 mg. thorium can be estimated with accuracy. Since ceric salts and cerite earths do not react with 1-hydroxy-3-methoxy xanthone, their separation from thorium presents no difficulty. It has been found that 10·0 mg. thorium can be separated from a ten-fold excess of cerite earths and five-fold excess of ceric salts. Uranium also does not get precipitated in this pH range. With a single precipitation a seven-fold excess of uranium salts can be separated. A very large excess (upto fifteen times) of uranium can be separated using double precipitation. For the estimation of thorium or for its separations from the above elements, sulphate ions should not be present in the solution, since complex formation is totally inhibited by them. The estimation can be smoothly carried out in the presence of chloride and nitrate ions.

Experimental

Reagents

(*a*) *Thorium nitrate solution.*—Thorium nitrate (B.D.H.) was purified by the method of Rao and Patel.[20] The thorium content of the solution was determined by the 8-hydroxy-quinoline method.

(*b*) 1-*hydroxy*-3-*methoxy xanthone.*—It was prepared by the condensation of phloroglucinol-dimethyl ether[21] with salicylic acid in presence of fused zinc chloride.[22] A 2% (almost saturated) solution of the xanthone in alcohol was used.

(*c*) Other reagents used were of A.R. quality.

Procedure for precipitation

To an aqueous thorium nitrate solution (pH adjusted) containing about 0·1 g. of thorium in about 100 c.c., alcohol (30 c.c.) was added. The mixture was heated on a water-bath nearly to boiling and an excess (40–50 c.c.) of the xanthone solution in alcohol was added. The deep yellow solution obtained was heated on a water-bath to remove most of the alcohol. It was then cooled and water (100 c.c.) added when all the thorium complex was precipitated. The flocculent precipitate was filtered and washed repeatedly with water. It was then dried at 120° and ignited in a weighed platinum crucible to constant weight (ThO_2). As the precipitate is voluminous, it is not convenient to take quantities larger than 0·1 g. of thorium. Smaller quantities could be used without any modification in the procedure.

Relative amount of the xanthone required for precipitation

As shown below, the complex formed contains four xanthone units attached to a thorium atom. In order to effect complete precipitation,

therefore, at least six moles of xanthone should be added for each mole of the thorium salt. It is desirable however to add larger proportions of the xanthone.

Effect of pH on the precipitation of thorium

The effect was studied by buffering thorium nitrate solutions with sodium acetate-hydrochloric acid mixture and then precipitating the complex. As thorium salts tend to hydrolyse above pH 4·0 the effect was studied only upto this pH. Precipitation of solutions containing 20·00 mg. of thorium oxide was carried out at different pH values. There was no precipitation below pH 1·0 and it increased upto pH 2·6 when it was complete and continued to be complete upto pH 4·0. Beyond pH 3·5 the procedure for precipitation had to be modified because thorium nitrate underwent hydrolysis on boiling. 1-Hydroxy-3-methoxy xanthone was added in this case in the cold. After about five minutes of thorough stirring the solution was heated on a water-bath to remove the alcohol. Complete removal of alcohol is very necessary as otherwise some of the complex passes through the filter-paper in the colloidal state. The precipitate was then filtered, washed, dried and heated as before.

It could be seen from the above observations that the most convenient range for estimating thorium is 2·6–3·5. In order to avoid any possibility of hydrolysis the most desirable conditions were in the pH range 2·6–3·2.

Molar composition of the complex

X c.c. of xanthone solution ($1{\cdot}25\times10^{-3}$ M) were mixed with (10 − X) c.c. of thorium solution of the same molarity and the value of X varied from 1 to 9. Optical densities of these mixtures were determined at 400 $m\mu$ employing the xanthone solution as blank. The absorption due to the reacting solutions is small at that wave-length and at the same time the absorption of the complex is maximum (see Fig. 1). The difference between the optical density of the complex and of the reactants, therefore, is the same as the optical density of the complex itself in this case. The values of the optical densities (called the Y value) for the different mixtures were plotted against X. The curve showed a peak when the molar ratio was 8 : 2. The complex should, therefore, have the formula ThL_4, where L represents a unit of the xanthone.

Separation of thorium from cerite earths and ceric salts

Since 1-hydroxy-3-methoxy xanthone does not react with cerite earths and ceric salts, it can be used for separating thorium from these elements,

The experimental results obtained are given in Table I. All precipitations were carried out at pH 2·8.

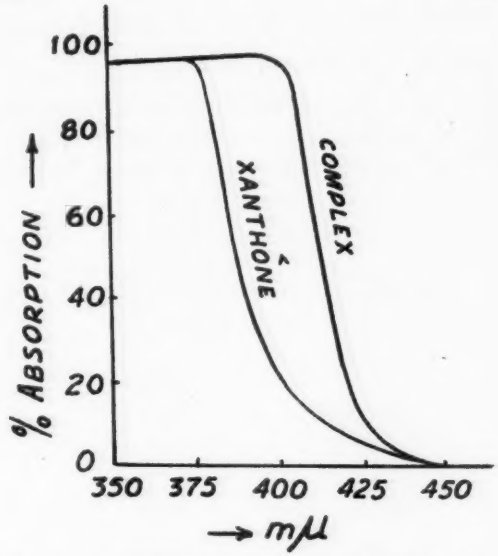

FIG. 1. Absorption of the Reagent and the Complex.

TABLE I

S. No.	ThO_2 (taken as thorium nitrate)	Ceric salts present	Cerite earths present	ThO_2 obtained after precipitation with the xanthone
	mg.	mg.	mg.	mg.
1	50·00	50·00	..	50·02
2	50·00	..	50·00	50·03
3	50·00	50·00	50·00	50·03
4	25·00	50·00	50·00	25·02
5	10·00	10·00	10·00	10·01
6	10·00	20·00	20·00	10·02
7	10·00	50·00	20·00	10·12
8	10·00	50·00	50·00	10·14
9	10·00	100·00	50·00	10·30
10	10·00	50·00	100·00	10·10

It was found that 10·00 mg. thorium can be separated with a fair degree of accuracy from a five-fold excess of ceric salts and ten-fold excess of cerite earths. The results become somewhat erroneous, however, if the quantity of ceric salts is more than five times the amount of thorium salt.

Separation of thorium from uranium (uranyl salts)

Uranyl salts react with 1-hydroxy-3-methoxy xanthone only at comparatively higher pH and hence do not interfere in the thorium estimation. The results obtained for this separation are given in Table II.

TABLE II

S. No.	ThO_2 (taken as thorium nitrate)	U_3O_8 (taken as uranyl nitrate)	ThO_2 found
	mg.	mg.	mg.
1	50·00	100·00	50·01
2	20·00	100·00	20·02
3	20·00	150·00	21·03
4	20·00	150·00	*20·03
5	20·00	200·00	*20·02
6	10·00	100·00	*10·02
7	10·00	200·00	*10·12

* Double precipitation employed.

A single precipitation with 1-hydroxy-3-methoxy xanthone can separate uranium as much as nearly five to six times the amount of thorium. For separating larger quantities of uranium, the precipitate obtained was heated with concentrated nitric acid to decompose the organic matter. Most of the acid was slowly evaporated off and the solution was again restored to pH 2·8–3·2 and thorium was reprecipitated. With the double precipitation a fifteen-fold excess of uranium could be separated from as little as 20·0 mg. of thorium.

SUMMARY

1-Hydroxy-3-methoxy xanthone forms a complex ThL_4 in aqueous alcoholic solution at pH 2·6–4·0 and it can be precipitated with water, dried

and ignited to yield thorium dioxide. This provides a satisfactory method of estimation of the metal in the presence of a large excess of cerite earths and ceric salts since these are not precipitated by this reagent and also in the presence of uranium which gets precipitated only at higher pH. The method can be used for separation also.

References

1. Kaufmann .. *Trav. inst. état radium*, 1938, **4**, 313.
2. Wenger and Duckert *Helv. Chem. Acta*, 1942, **25**, 1547.
3. Osborn .. *Analyst*, 1948, **73**, 381.
4. Willard *et al.* .. *Anal. Chem.*, 1949, **21**, 1323.
5. Rao and Rao .. *J.I.C.S.*, 1950, **27**, 457.
6. Murty and Rao .. *Ibid.*, 1950, **27**, 459.
7. Venkateswarlu and Rao *Ibid.*, 1950, **27**, 638.
8. Murty and Rao .. *Ibid.*, 1951, **28**, 218.
9. Wengert *et al.* .. *Anal. Chem.*, 1952, **24**, 1636.
10. Krishnamurty and Purshottam *Rec. Trav. Chim.*, 1952, **71**, 671.
11. Datta and Banerjee .. *J.I.C.S.*, 1955, **32**, 231.
12. Ryan *et al.* .. *Anal. Chem.*, 1947, **19**, 416.
13. Rao *et al.* .. *J.I.C.S.*, 1950, **27**, 610.
14. Krishnamurthy and Rao *Rec. trav. Chim.*, 1951, **70**, 421.
15. Venkateswarlu *et al.* .. *J.I.C.S.*, 1950, **27**, 638.
16. Venkataramiah *et al.* *J. Sci. Ind. Res.*, 1951, **10 B**, 254; *Anal. Chem.*, 1952, **24**, 747.
17. Rao and Rao .. *Z. anal. Chem.*, 1954, **142**, 27.

17*a*. Saxena and Seshadri .. *Proc. Ind. Acad. Sci.*, 1957, **46 A**, 218.

18. Job .. *Ann. Chim.*, 1928, **9**, 113.
19. Vosburgh and Cooper *J. Amer. Chem. Soc.*, 1941, **63**, 437.
20. Rao and Patel .. *Proc. Ind. Acad. Sci.*, 1955, **42 A**, 317.
21. Pratt and Robinson .. *J.C.S.*, 1924, **125**, 188.
22. Mittal and Seshadri .. *J. Sci. Ind. Res.*, 1955, **14 B**, 76.

HETEROCYCLIC COMPOUNDS

Part XIII.* Synthetic Experiments in Furoquinolines

By P. S. Raman

(Department of Organic Chemistry, University of Madras, Madras-25)

Received December 11, 1957

(Communicated by Dr. K. N. Menon, F.A.SC.)

The linear furoquinoline ring system is of great interest because of its presence in dictamnine (I *a*) and other alkaloids occurring in plants of the Rutaceæ family.[1] In view of the recent publications[2–4] on the synthesis of dictamnine and γ-fragarine (I *b*), the results of some of the work carried out in this laboratory towards the synthesis of linear furoquinolines are reported in this communication.

An attractive route for the synthesis of furoquinolines seemed to be through appropriately substituted quinoline-3-acetic acids. As a first step, 4-methyl-1, 2-dihydro-2-oxoquinoline-3-acetic acid (II), because of its ready availability, was chosen. The synthesis of this acid has been reported from this laboratory in a previous communication.[5] The ethyl ester (III), on reduction with lithium aluminium hydride, gave 3, 2′-hydroxyethyl-4-methyl-1, 2-dihydro-2-oxoquinoline (IV). The reduction gave some practical difficulties because of the very poor solubility of the ester in solvents like ether and dioxan. The alcohol was finally obtained in very good yields by adding the solid ester to a stirred suspension of the hydride in a very large volume of ether and continuing the stirring for five to six hours with refluxing. The alcohol (IV) showed properties typical of a 2-quinoline; it was insoluble in dilute acids and dilute caustic alkali and gave an yellowish colour with ferric chloride in ethanol. When (IV) was suspended in dry chloroform containing a small quantity of pyridine and treated with thionyl chloride, it afforded a chlorine-free product, freely soluble in dilute acids. This proved to be 4′, 5′-dihydro-4-methyl-furano (2′, 3′-2, 3)-quinoline (V), the cyclisation having probably proceeded through the intermediate 3, 2′-chloroethyl-4-methyl-1, 2-dihydro-2-oxoquinoline (VI). It was also found that the cyclisation of (IV) to (V) could be more smoothly effected by the use of polyphosphoric acid.

---

* Part XI.

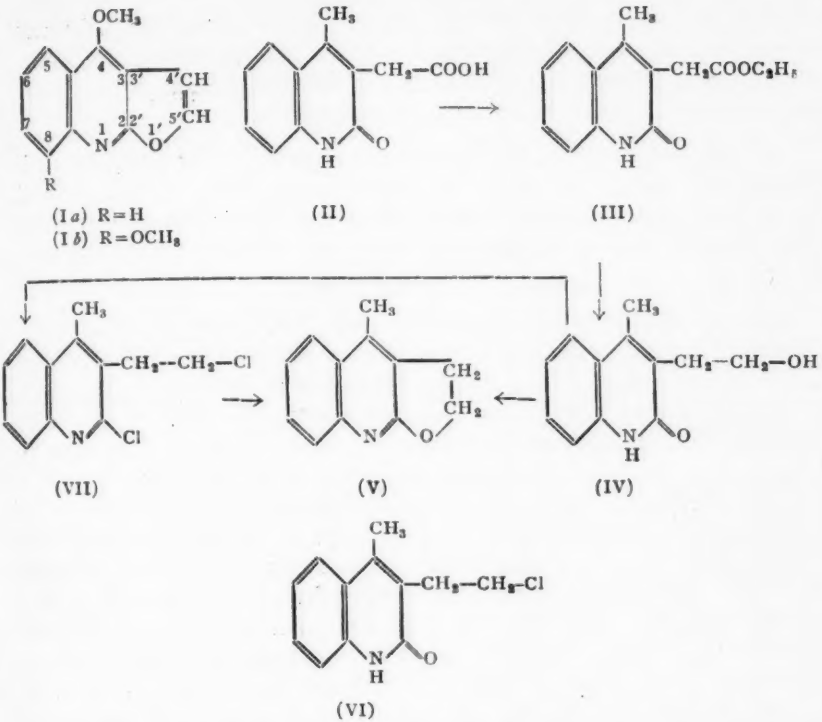

(I *a*) R = H
(I *b*) R = OCH_3

(II)

(III)

(VII)

(V)

(IV)

(VI)

The chlorine in many 2-chloroquinolines has been shown to be extremely labile. Thus 4, 7-dichloro-1, 2-dihydro-2-oxoquinoline has been obtained[6] in good yields by acid hydrolysis of 2, 4, 7-trichloroquinoline. Grundon and McCorkindale[4] converted 2, 4-dichloro-3, 2′-chloroethyl-quinoline into the corresponding 2-quinoline. It was thus thought possible to convert 2-chloro-3, 2′-chloroethyl-4-methyl-quinoline (VII), prepared from (IV) or (V) by treatment with $POCl_3$, into the monochloro compound (VI) under the same conditions of hydrolysis. The compound (VI) could then be easily cyclised to (V). It was rather a surprise to find that the hydrolysis could not be effected, the starting material being recovered back. This led to examining the hydrolysis 2-chloro-4-methyl-quinoline and 2-chloro-3-ethyl-4-methyl-quinoline. It was found that while the former gave a very high yield of 4-methyl-carbostyril, the latter compound which is more closely related to (VII), gave only a very poor yield of the known 3-ethyl-4-methyl-carbostyril. The recent report[7] that 2, 4-dichloro-3-dichloromethyl-quinoline could be converted into 4-chloro-3-dichloromethyl-1, 2-dihydro-2-oxoquinoline by

just refluxing with glacial acetic acid gives added interest to the differences exhibited by the 2-chloro-quinolines towards acid hydrolysis. Evidently, the substituents present in the pyridine part of the molecule have a great effect on the hydrolysability of 2-chloro compounds.

The dehydrogenation of (V) into the corresponding furoquinoline with palladium on carbon has not been so far successful. Grundon and McCorkindale[4] report that they could effect the dehydrogenation of their dihydro-furoquinoline with palladium on carbon only in 5% yield (see also reference 15).

Dihydrobenzofurans are readily obtained from *o*-allyl-phenols. Since this method has not so far been applied for the preparation of dihydrofuro-(2′, 3′-2, 3)-quinolines, it was thought profitable to investigate this route. The starting material used was α-allyl-acetoacetanilide (IX) obtained by condensing sodio-acetoacetanilide (VIII) with allyl bromide. The expectation was to cyclise this to 3-allyl-4-methyl-1, 2-dihydro-2-oxoquinoline (XI) and then convert the latter to the dihydro-furoquinoline. When (IX) was treated with polyphosphoric acid, it gave rise to a product which did not show the properties of a 2-quinolone. It was freely soluble in dilute acids and proved to be 4′, 5′-dihydro-4, 5′- dimethyl-furano (2′, 3′-2, 3)-quinoline (X); the —OH in the 2-position of (XI) having added to the double bond of the allyl side chain. This formulation is consistent with Markovinikov's rule as well as the results of Hurd and Hoffman[8] on *o*-allyl phenols. The alternate possible structure (XII) for the final product is ruled out on the basis of the absorption spectra of the compound. The dihydro-furoquinoline (X) could not also be dehydrogenated using palladium on carbon.

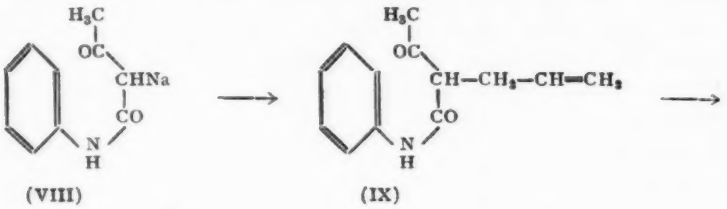

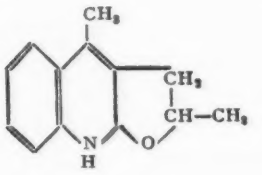

(X)

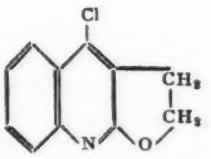

(XIII)

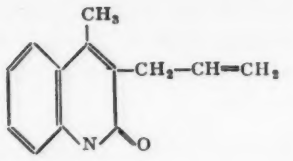

(XI)

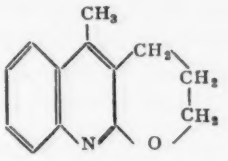

(XII)

The U.V. absorption spectra curves of (V) and (X) are identical (see Fig. 1). They are also similar to the U.V. absorption curve for 4-chloro-4', 5'-dihydrofurano (2', 3'-2, 3) quiinoline (XIII) reported by Grundon and McCorkindale.[4] The relevant absorption maxima are:

	λ	ε	λ	ε	λ	ε
Substance X	272	5074	312	5589	326	6279
V	272	5039	312	5363	326	5936

Both the curves show a characteristic bifurcation of one peak (see figure). Although this bifurcation is exhibited by 2-quinolones,[9] it has been noticed[4] that dihydrofurano (2', 3'-2, 3) quinolines and other quinolines having an

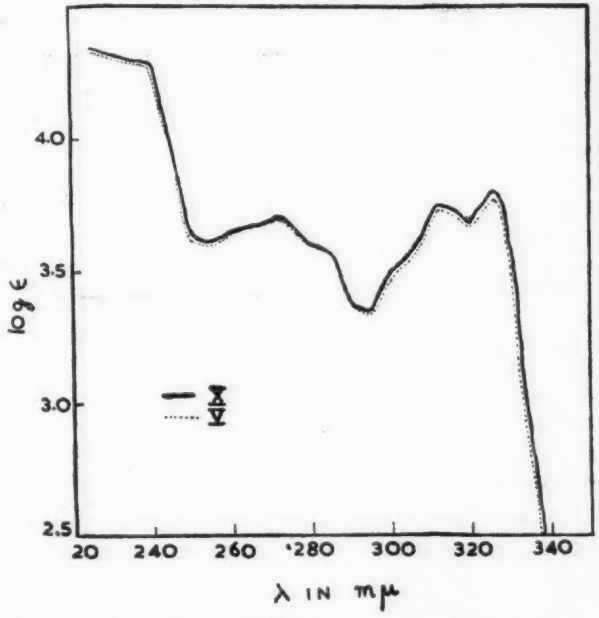

FIG. 1. U.V. Spectra of Substances V and X (in 95% ethanol)

ether function at the 2-position show some of the characteristics of 2-quinolones in their U.V. spectra. The greater intensities at 312 $m\mu$ and at 326 $m\mu$ in the case of (X) may probably be due to the influence of the second methyl group present in the oxygenated ring.

The infra-red spectra of (V) and (X) also show close resemblances (see Fig. 2). Here also some of the characteristics of 2-quinolones is exhibited by these compounds. The amide-carbonyl in 2-quinolones gives a characteristic I.R. band between 1660 and 1640 cm.[4, 10–12] The I.R. spectra of (V) and (X) show a fairly intense band in the 1630 cm.$^{-1}$ region. Grundon and McCorkindale[4] also report similar absorption for their dihydrofuranoquinolines.

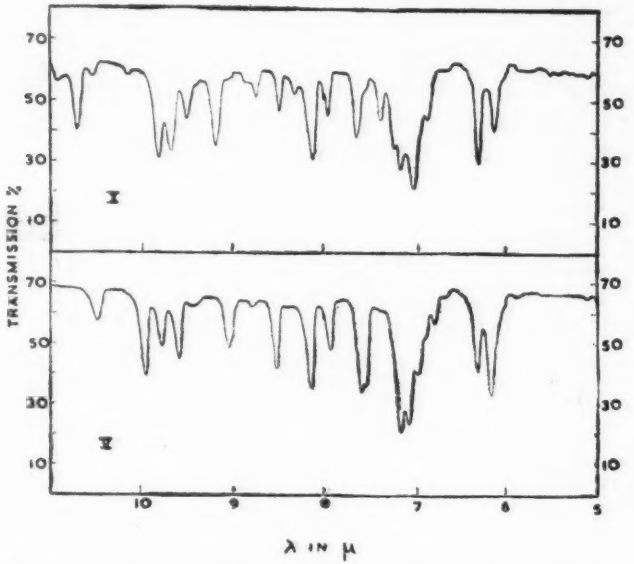

FIG. 2. I.R. Spectra of Substances V and X (as solid in KBr).

EXPERIMENTAL

Ethyl 4-*methyl*-1, 2-*dihydro*-2-*oxo*-*quinoline*-3-*acetate* (*III*)

This was obtained from the corresponding acid (II)[6] by ethanol-sulphuric acid esterification and crystallised from ethanol in feathery needles, m.p. 220–22°.

3, 2'-*Hydroxyethyl*-4-*methyl*-1, 2-*hydro*-2-*oxo*-*quinoline* (*IV*)

In a one litre three-necked flask, provided with a mercury-sealed stirrer and reflux condenser, were placed lithium aluminium hydride (1·8 g.) and absolute ether (600 ml.). The previously vacuum-dried ester (III, 3·6 g.) was introduced in three portions through the third neck of the flask, while the mixture was kept well stirred. After an hour at room temperature, the mixture was gently refluxed for five hours under stirring. It was then allowed to stand at room temperature for about 18 hours. The excess of the metallic hydride was destroyed by the addition of a little ethyl acetate, the flask cooled in ice and the complex decomposed with ice and dilute hydrochloric acid. The clear upper ether layer was decanted and the solid sticking to the sides of the flask was collected, washed with water, dried and crystallised from ethanol (charcoal) in rosettes of needles, m.p. 217–18° (Yield 2·2 g.; 74%). It was insoluble in dilute sodium hydroxide and gave an yellowish colour with alcoholic ferric chloride.

Found:	C, 70·6	H, 6·85
$C_{12}H_{13}O_2N$ requires	C, 70·8	H, 6·45

4-*Methyl*-4', 5'-*dihydrofurano* (2', 3'-2, 3) *quinoline* (*V*)

Method a.—The alcohol (IV; 1·5 g.) was added to a mixture of dry chloroform (30 ml.) and pyridine (0·4 ml.) and then treated with thionyl chloride (4 ml.). The mixture immediately warmed up and a clear solution was momentarily formed; but soon a solid began to separate out. After allowing to stand at room temperature for 15 minutes, the mixture was refluxed on the water-bath for the same time. The solvent and excess of thionyl chloride was removed at the water pump and the residue treated with water (125 ml.) containing a small quantity of hydrochloric acid. The solution was filtered and basified with ammonia, under cooling. The fine precipitate was collected, washed with water and dried (m.p. 119–21°, 1·2 g.–86%). Crystallised from light petrol, it formed colourless needles of m.p. 123–24°; soluble in alcohol, benzene and carbon tetrachloride.

Found:	C, 77·3	H, 5·8
$C_{12}H_{11}ON$ requires	C, 77·8	H, 5·95

The picrate crystallised from ethanol in long, yellow needles of m.p. 195–96°.

Found:	C, 52·0	H, 3·9
$C_{12}H_{11}ON$, $C_6H_3O_7N_3$ requires	C, 52·2	H, 3·4

Method b.—To polyphosphoric acid prepared from phosphorous pentoxide (10 g.) and phosphoric acid (6 ml.) was added the alcohol (IV, 1·2 g.). The mixture was heated on the water-bath for five hours with the exclusion of moisture. After cooling, the viscous product was poured on to ice and water under efficient stirring. The solution was filtered and basified with ammonia, yielding the same product as under Method *a* but in a purer form (1·05 g.). It formed plates from dilute ethanol, m.p. 123–24° and showed no depression on admixture with the product from Method *a*.

2-Chloro-3, 2'-chloroethyl-4-methyl-quinoline (VII)

The alcohol (IV, 0·5 g.) and phosphorous oxychloride (4 ml.) were heated in an oil-bath at 120–25° for 3½ hours. The excess of oxychloride was then removed at the water pump, and the residue treated with ice and water. The solid (0·55 g., m.p. 134–36°) crystallised from ethanol in stout rods, m.p. 137–39°.

Found:	C, 59·7	H, 4·6
$C_{12}H_{11}Cl_2N$ requires	C, 60·0	H, 4·6

The chloro compound (VII, 0·15 g.) was refluxed with 6 N hydrochloric acid (5 ml.) and dioxan (4 ml.) for 3 hours. After standing overnight, it was diluted with water (12 ml.) yielding the original compound. In another experiment the compound (VII, 0·1 g.) was refluxed for 3 hours with concentrated hydrochloric acid (3 ml.). On dilution with water the unchanged material was recovered.

Acid hydrolysis of 2-chloro-4-methyl-quinoline

A mixture of 2-chloro-4-methyl-quoinline (1 g.), 6 N hydrochloric acid (28 ml.) and dioxane (22 ml.) was refluxed for 3 hours. On standing overnight a crystalline solid separated. It was collected, washed with water and on drying melted at 220–22°. Its identity with 4-methyl-carbostyril was established by mixed melting point, no depression taking place.

Acid hydrolysis of 2-chloro-3-ethyl-4-methyl-quinoline[18]

A gram of the compound was treated as above. As no product separated on allowing the reaction mixture to stand for 12 hours, it was diluted with an equal volume of water. There was still no precipitation. Treatment with solid sodium carbonate yielded a solid (0·95 g.). It was triturated with cold ethanol (15 ml.) and the residue (0·1 g.) collected. It melted at 226–28°, showing no depression when mixed with 3-ethyl-4-methyl

carbostyril. The alcoholic filtrate yielded (0·8 g.) of the original chloro compound.

α-Allyl-acetoacetanilide (IX)

To a hot solution of acetoacetanilide (8·8 g.; 1 mole) in absolute benzene (100 ml.) was added molecular sodium (1·15 g.; 1 atom). The formation of the sodium salt was completed by refluxing for 6–7 hours, and it was then treated with allyl bromide (4·5 ml.; slight excess) in dry benzene (10 ml.). After standing overnight, it was refluxed for 5 hours, cooled and treated with ice water. The benzene layer was separated, washed with water, dried over anhydrous sodium sulphate, and benzene removed to yield a viscous liquid (8·6 g.). This was taken up in boiling light petrol and then cooled when the anilide separated in clusters of needles (6·5 g.; m.p. 72–75°). Recrystallised from the same solvent, m.p. 79–80°.

Found:	C, 72·2	H, 7·3
$C_{13}H_{15}O_2N$ requires	C, 71·9	H, 6·9

4′, 5′-Dihydro-4, 5′-dimethyl-furano (2′, 3′-2, 3) quinoline (X)

The crude allyl acetoacetanilide (from 8·8 g. of acetoacetanilide) was added to polyphosphoric acid prepared from phosphorous pentoxide (20 g.) and phosphoric acid (12 ml.). The mixture warmed up and the anilide went into solution. After heating for 2 hours on the water-bath, the mixture was cooled, poured on to crushed ice and stirred well. A small quantity of sticky material that separated out was removed by filteration and the solution basified with ammonia. Solution in acid and reprecipitation was found advantageous. The product (5·0 g.; 51% on the wt. of acetoacetanilide) was soluble in benzene and carbon tetrachloride but insoluble in light petrol and formed colourless needles from dilute ethanol, m.p. 119–20°.

Found;	C, 78·3; 78·5	H, 6·5; 6·5
$C_{13}H_{13}ON$ requires	C, 78·4	H, 6·5

The picrate was obtained in golden yellow plates from ethanol, m.p. 195–97°.

Found:	C, 53·7	H, 4·1
$C_{13}H_{13}ON$, $C_6H_3O_7N_3$ requires	C, 53·3	H, 3·7

Attempted dehydrogenation of (V) and (X)

The dehydrogenation was attempted in boiling *p*-cymene, α-methyl naphthalene and diphenyl ether in different experiments. Both 10% and

30% palladium on charcoal were tried. In all cases practically the whole of the starting material was recovered unchanged. On prolonged boiling in diphenyl ether, the solution assumed a slight greenish-blue fluorescence, but no dehydrogenated product could be isolated. Furo (2′, 3′ -2, 3) quinolines are reported[14] to show a blue-violet fluorescence in organic solvents.

SUMMARY

The synthesis of 4′, 5′-dihydro-4-methyl furano (2′, 3′-2, 3) quinoline and 4′, 5′-dihydro-4, 5′-dimethyl furano (2′, 3′-2, 3) quinoline are reported. Attempts at dehydrogenation of these compounds with palladium on carbon failed. The stability to acid hydrolysis of some substituted 2-chloro-quinolines is discussed.

ACKNOWLEDGEMENT

The author is grateful to Dr. K. N. Menon for his constant help and guidance in this work. Thanks are also due to Dr. Gurubakshi Singh of the National Physical Laboratory, Delhi, for the infra-red spectra; to Dr. D. Ramaswamy of the Central Leather Research Institute, Madras, for the ultra-violet spectra; and to Drs. Weiler and Strauss, Oxford, for some of the microanalyses reported here. Grateful acknowledgement is made to the Kerala University for a scholarship.

This work was carried out during the period of study leave granted to the author by the authorities of the Maharaja's College, Ernakulam.

REFERENCES

1. Openshaw, H. T. .. *The Alkaloids*, Vol. III. Editors: Manske and Holmes (Academic Press), 1953, p. 69.
2. Tuppy, H. and Bohm, F. *Ang. Chemie*, 1956, **68**, 388; *Monatsh*, 1956, **87**, 720, 774.
3. Sato, T. and Ohta, M. *J. Chem. Soc. (Japan)*, 1956, **77**, 1630.
4. Grundon, M. F. and McCorkindale, N. J. *Chem. and Ind.*, 1956, 1091; *J. Chem. Soc.*, 1957, 2177.
5. Raman, P. S. .. *Proc. Ind. Acad. Sci.*, 1957, **45**, 260.
6. Rowlett, R. J. and Lutz, R. E. *J. Amer. Chem. Soc.*, 1946, **68**, 1288.
7. Sato, T. and Ohta, M. *Bull. Chem. Soc. Japan*, 1956, **29**, 817.
8. Hurd, C. D. and Hoffman, W. A. *J. Org. Chem.*, 1940, **5**, 212.
9. Witkop, B., Patrick, J. B. and Rosenblum, M. *J. Amer. Chem. Soc.*, 1951, **73**, 2644.

10. Gibson, J. A., Kynaston, W. and Lindsey, A. S. — *J. Chem. Soc.*, 1955, 4340.

11. Cook, D. J. Yunghans, R. S., Moore, T. R. and Hoogenboom, B. E. — *J. Org. Chem.*, 1957, **22**, 211.

12. Grundon, M. F., McCorkindale, N. J. and (in part) Rodger, M. N. — *J. Chem. Soc.*, 1955, 4284.

13. Searles, A. L. and Lindwall, H. G. — *J. Amer. Chem. Soc.*, 1946, **68**, 988.

14. Ohata, T. and Mori, Y. — *Pharm. Bull.* (*Japan*), 1956, **4**, 415.

15. Price, J. R. — *Fortschr. Chem. Org. Naturstoffe*, 1956, **13**, 321.

EFFECT OF METHYL ORANGE ON THE CAPACITY OF THE DROPPING MERCURY ELECTRODE

By S. L. Gupta

(Physico-Chemical Laboratories, Birla College of Science, Pilani, Rajasthan)

Received December 17, 1957

(Communicated by Dr. K. S. G. Doss, F.A.SC.)

1. Introduction

The first detailed investigation of the effect of surface-active substances on the capacity of the dropping mercury electrode was made by Proskurnin and Frumkin.[1] Their experiments showed the existence of two maxima with a strong depression in the middle part in the capacity-potential curve of sodium sulphate saturated with octyl alcohol. These features were confirmed by the more precise measurements of Grahame.[2] The pulsating field technique as modified by Doss and Kalyanasundaram is found to be very convenient for the investigation of these phenomena.[3] Breyer and Hacobian have also used a similar technique for such investigations.[4] The earlier papers have shown how surface-active substances influence the dropping mercury electrode capacity by getting adsorbed at the mercury-aqueous interface.[5] At some of the applied D.C. potentials the capacity is also affected due to a dynamic contribution from the sorption and desorption processes which occur due to the pulsating field applied for measuring the capacity.

The present work relates to the effect of methyl orange on the capacity of the dropping mercury electrode under different conditions of pH and concentration. One distinguishing feature of this work is that the surface-active substance is a chemical compound of known structure and can be purified easily by crystallisation from its aqueous solution.

2. Experimental

2.1. Methyl Orange used was Merck's quality and recrystallised twice before use.

2.2. The mercury used for pool-electrode and dropping electrode was passed through Meyer's column, washed several times with distilled water, dried and passsd through a sintered glass filter.

2.3. The other chemicals used were of 'Analar' quality of B.D.H.

2.4. *Technique of Measurement.*—The apparatus employed in the present investigation is the same as what has been described before.[3, 5a] This consists in applying to a dropping mercury electrode, 50 cycles A.C. ripple of $\pm$ 45 mv. (r.m.s.) over the D.C. potential and observing the alternating component of the resulting pulsating current. As the capacitative impedance of the dropping mercury electrode is much higher than the rest of the impedance of the system, the magnitude of the alternating current gives a measure of the dropping mercury electrode capacity. The D.C. potentials have been expressed with reference to the saturated calomel electrode. The constants of the dropping mercury electrode are as follows:—

$m = 0{\cdot}0037$ g./sec.

$t = 0{\cdot}7$ sec. per drop in 0·1 M KCL (open circuit).

0·1 Molar potassium chloride solution was used as the supporting electrolyte and was invariably shaken and kept in contact with mercury and mercurous chloride. In each case, the measurements were taken with the indifferent electrolyte and the effect of the surface-active substances has been expressed in terms of the percentage increase (with sign) of the alternating current, which gives practically the percentage increase in the average differential capacity. It has been shown by experiments that the percentage increase in the current brought about by surface-active substances of low molecular weight is independent of the size of the drop or even the time of the dropping within certain limits.[5d] The dropping mercury electrode was cathodic throughout the measurements.

The results are represented in Figs. 1–4.

3. Discussion

3.1. *Behaviour of Methyl Orange at pH* 12·3.—This system is distinguished by the occurrence of a main peak and a satellite at all concentrations examined from 0·0025% to 0·04% of methyl orange (*vide* Fig. 1). The satellite peak occurs at about 1·15 volts at all the concentrations studied. The main peak, however, changes its position and magnitude. As the concentration increases the peak tends to shift to more cathodic potentials. Furthermore, as the concentration increases, the magnitude of the peak diminishes at first and then increases to a high value.

In order to examine whether it is caused by any impurities present in the system, the methyl orange used was purified by repeated crystallisation. An examination of Fig. 4 shows that once recrystallised as well as twice recrystallised methyl orange behave in an identical manner. This shows

that the occurrence of the main and satellite peaks is a real phenomenon and not due to the effect of any impurity.

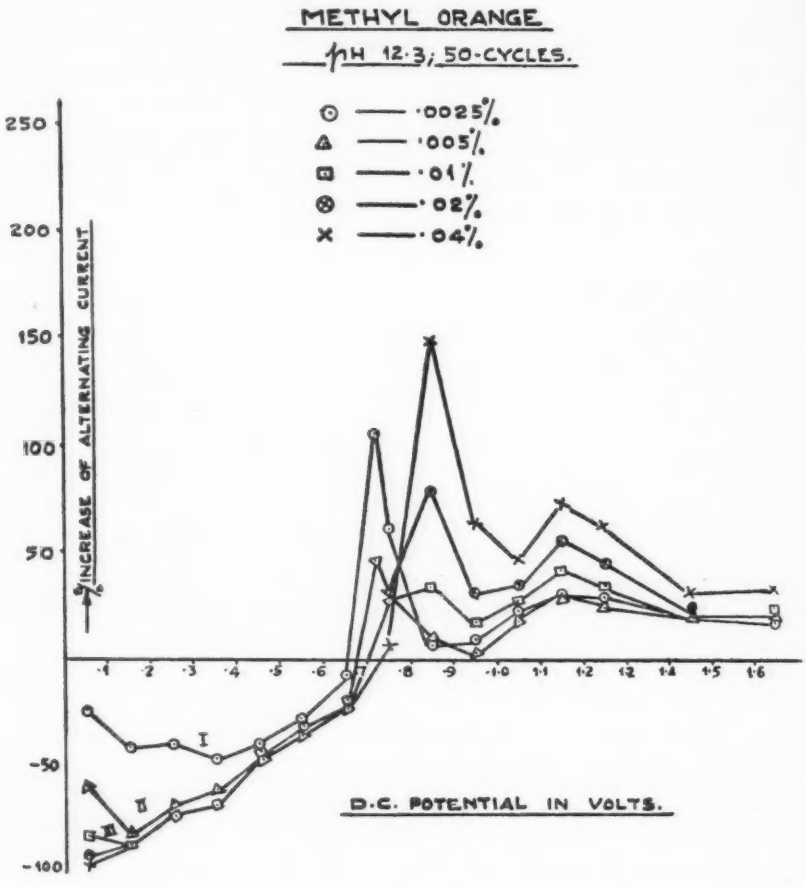

FIG. 1

The above results of extraordinary interest can be interpreted on the following hypothesis:—

The main peak is caused by the charge on the mercury surface converting the condensed film of adsorbed methyl orange into a vapour film, by a two-dimensional phase transition occurring more or less suddenly. The resulting vapour film is having a sufficiently high vapour pressure. The

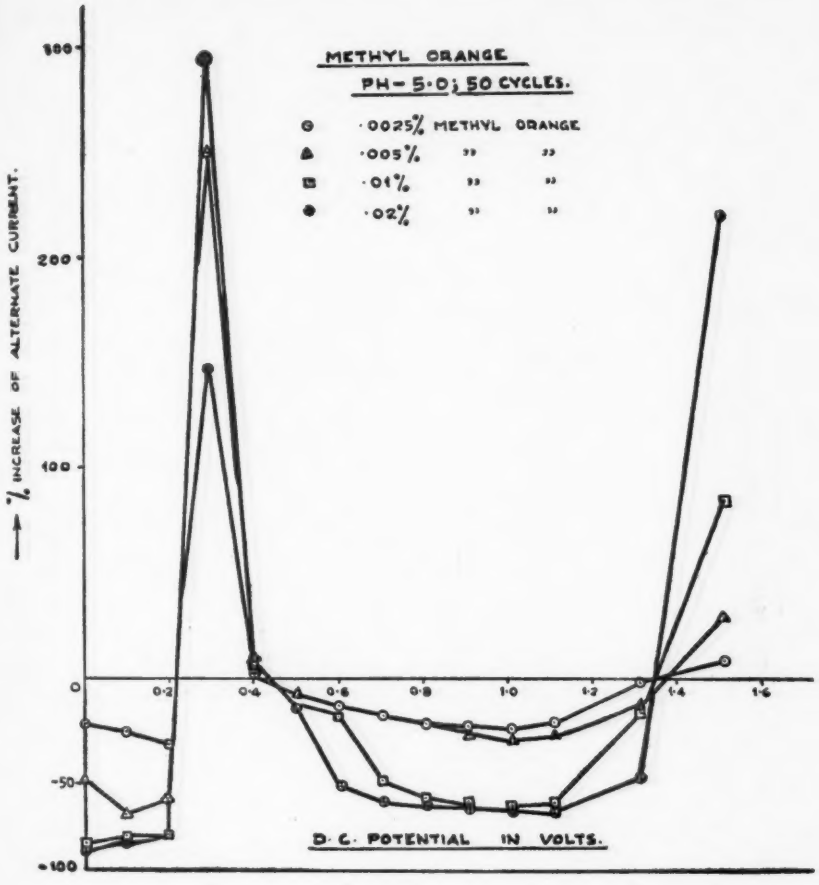

FIG. 2

satellite peak is caused by the complete desorption of the gaseous film at the higher voltage. The behaviour of the magnitude of the peak with changes of concentration of methyl orange is presumably connected with micelle formation. In very dilute solutions one is dealing with single molecule of methyl orange which can easily diffuse and have their full effect at the mercury solution interface. At intermediate concentrations, micelle formation sets in and brings down the rate of diffusion which lowers the magnitude of the peak. This goes up to 0·01% of methyl orange. At still higher concentrations the concentration of the micelle increases and hence the magnitude

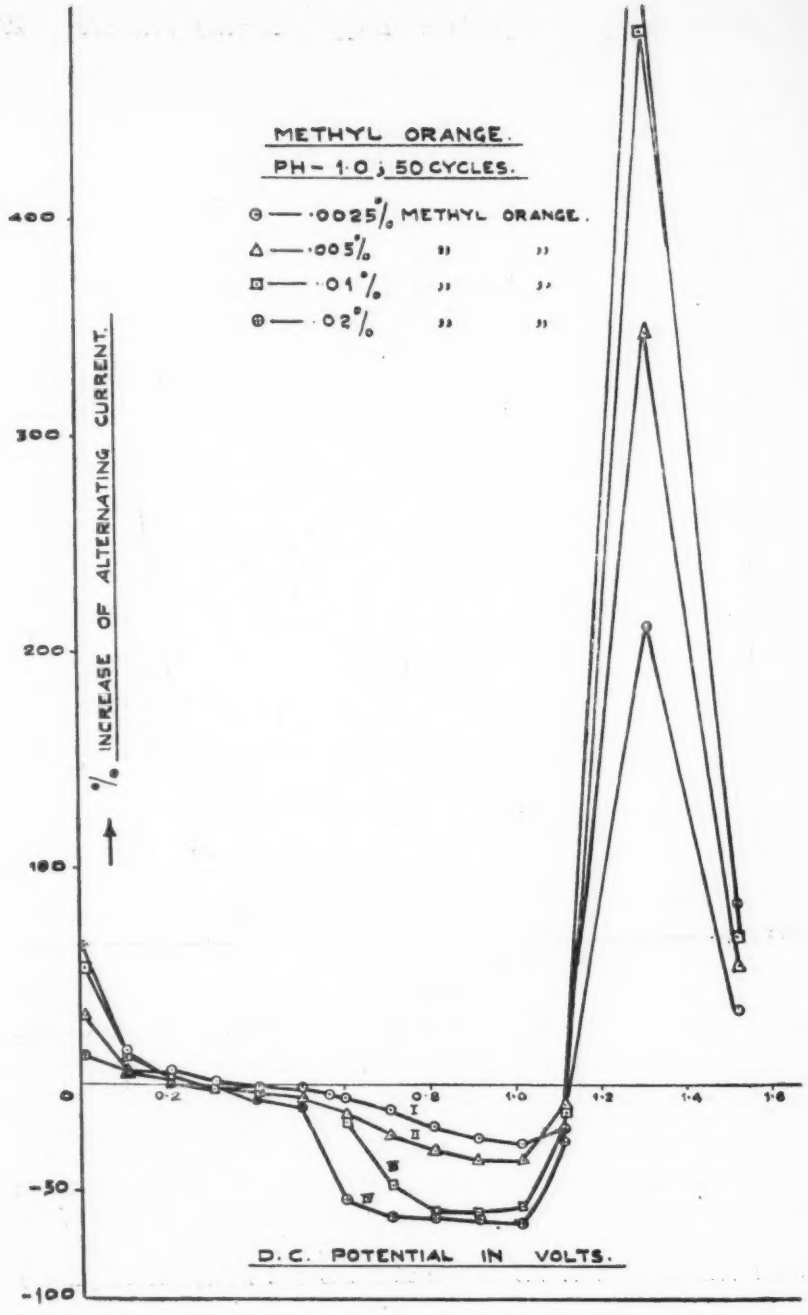
METHYL ORANGE.
PH – 1·0 ; 50 CYCLES.
⊙ — ·0025% METHYL ORANGE.
△ — ·005% " "
□ — ·01% " "
⊕ — ·02% " "
% INCREASE OF ALTERNATING CURRENT.
400
300
200
100
0
-50
-100
0·2
0·8
1·0
1·2
1·4
1·6
I
II
III
IV
D.C. POTENTIAL IN VOLTS.

FIG. 3

of the peak also increases. The effect of concentration of methyl orange and other surface-active substances on peak potential will be considered in a separate paper.

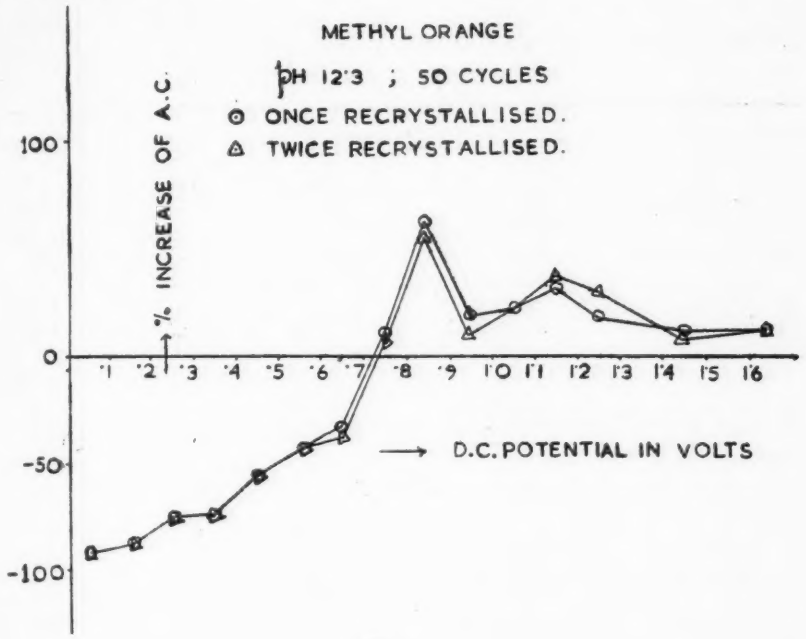

FIG. 4

3.2. *Behaviour of Methyl Orange at pH* 5·0.—The first important distinguishing feature at this pH value is the absence of the satellite peak. This is presumably due to the adsorptive forces being strong in the vapour film even after the phase transition, and a vapour film having a high concentration of the adsorbed molecules. This strongly adsorbed film appears not to get desorbed right up to a potential of 1·5 volts at which there is a peak due to the cathodic reduction of the substance.

In a separate paper[6] a method has been described which can be adopted for finding out generally whether the peak is due to desorption or reduction. In the present case it appears that the peaks observed at lower voltages are due to desorption whereas those at a cathodic potential of 1·3 volts or higher are chemical peaks due to reduction.

3.3. *Behaviour of Methyl Orange at pH* 1·0.—The desorption peak is now at zero volt or even at the anodic side. The satellite peak is absent.

TABLE I

Effect of pH on Peak Potential

	Substance used	Nature of peak	Peak potential at pH 1·0	Peak potential at pH 5·0	Peak potential at pH 12·3
		Class A			
			1·3	1·7	>1·7
1.	Methyl orange ..	Main peak ..	0	·3	·85
		Subsidiary peak	..	..	1·15
2.	Thymol blue ..	Main peak ..	<0	·65	·98
		Subsidiary peak	·5	1·1	..
3.	Bromocresol purple	Main peak ..	..	·55	·95
4.	Methyl blue ..	Main peak ..	·01	·2	·45
		Class B			
5.	Cetyl-pyridinium-bromide ..	Main peak ..	..	1·6 0	1·25 <0
		Class C			
			1·25	1·35	1·3
6.	Isopropyl alcohol	Main peak ..	·15	·15	·15
7.	Isobutyl alcohol	Main peak ..	1·25	1·35	1·3
			·1	·1	·15
8.	Benzene ..	Main peak ..	..	·9	·8
9.	Toluine ..	Main peak ..	..	·95	·9
10.	Amyl alcohol ..	Main peak ..	..	1·2	1·0
11.	Ether ..	Main peak ..	..	1·1	1·2
12.	Camphor ..	Main peak ..	..	1·2	1·3
13.	Lisapol ..	Main peak ..	..	1·7	1·65
				0	<0
		Negative peak ..	..	·9	·95
14.	Cerfak ..	Main peak ..	..	1·37	1·4
		Negative peak ..	..	·85	0·9
				·1	0
15.	Aerosol O.T. ..	Main peak ..	..	1·37	1·4
				·1	0
		Negative peak ..	..	·85	·9
16.	Lauryl-*p*-toluidine 2-sodium sulphonate	Main peak ..	..	1·35	1·4
		Negative peak ..	..	·85	·7
17.	Methyl violet ..	Main peak ..	1·31	1·34	..
18.	Methylene blue ..	Main peak ..	1·21	1·4	1·37

The absence of the satellite peak and other features can be interpreted as has been done in the case of pH 5·0. The peak at 1·3 volts is definitely a chemical peak caused by the cathodic reduction.

3.4.—*Effect of pH on a Peak Potential.*—The peak potentials whether it is of main peaks or subsidiary peaks get displaced by the change in pH. It is of interest in this connection to examine the behaviour of all the substances so far tried. Table I shows the summary of the results. The substances tried may be classified into three groups. Class A, comprising of methyl orange, thymol blue, bromocresol purple and methylene blue, shows a considerable shift towards more cathodic potentials with increase in pH. Class B, represented by cetylpyridinium bromide, shows a shift to less cathodic potentials at high pH. Class C, comprising of large number of substances, shows only a small shift in pH. No simple characteristic of these substances can be correlated with the present facts, but wherever the shift takes place, the whole curve appears to shift to the left or to the right. This indicates that the shift is due to the shift of the electro-capillary zero caused by these surface-active substances to different extents in different media.

There appears to be no interference by micelle formation at pH 1 or at pH 5·0. It may be that the micelle formation starts at much lower concentration at these pH values owing to high lateral adhesion.

4. Summary

The study of the behaviour of methyl orange at the dropping mercury electrode has revealed many new and interesting features. The most important feature is the presence of the main as well as satellite desorption peaks at pH 12·3 and absence of the satellite peaks at pH 5·0 and 1·0. The causes of this have been discussed in this paper. It has also been observed that at pH 12·3, the main peak changes its magnitude which indicates micelle formation.

5. Acknowledgement

The author wishes to thank Prof. K. S. G. Doss, D.Sc., F.R.I.C., F.Inst.P., F.A.Sc., F.N.I., Director, Central Electro-Chemical Research Institute, Karaikudi, for his valuable suggestions and discussions. Thanks are also due to Dr. S. M. Mitra, D.Sc., Principal, Birla College, Pilani, and Dr. R. D. Gupta, Ph.D., A.R.I.C., Head of the Chemistry Department, Birla College, Pilani, for their kind interest in the work.

6. REFERENCES

1. Proskurnin and Frumkin — *Trans. Far. Soc.*, 1935, **31**, 110.
2. Grahame .. *Am. Chem. Soc.*, 1946, **8**, 301.
3. Doss and Kalyanasundaram — *Proc. Ind. Acad. Sci.*, 1952, **35**, 27.
4. Breyer and Hacobian .. *Australian J. of Scientific Research*, Series A, 1952, **5**, 500.
5. (*a*) Doss and Gupta .. *Proc. Ind. Acad. Sci.*, 1952, **36**, 493.
   (*b*) Gupta .. *J. Sci. Ind. Res.*, 1953, **12 A**, 84.
   (*c*) ——— .. *Kolloid. Z.*, 1953, **132**, 21.
   (*d*) Doss and Gupta .. *Bull. Centr. Ele. Res. Instt., Karaikudi*, 1954, **1**, (2), 9.
   (*e*) Gupta .. *Proc. Ind. Acad. Sci.*, 1954, **39**, 282.
   (*f*) ——— .. *Kolloid. Z.*, 1954, **137**, 86.
   (*g*) ——— .. *Ibid.*, 1955, **141** 100.
   (*h*) ——— .. *Ibid.*, 1955, **141**, 102.
   (*i*) Doss and Gupta .. *Sci. and Cult.*, 1956, **22**, 102.
6. Gupta .. Unpublished.

350–58 Printed at the Bangalore Press, Bangalore City, by C. Vasudeva Rao, Superintendent, and Published by The Indian Academy of Sciences, Bangalore

ERRATA

(*Vol. XLVI, Nos.* 4 & 6, *October and December* 1957)

Page	*Line*	*For*	*Read*
251	25	these bands	the discrete bands
252	10	He	They
253	4 (from bottom)	were	was
264	1 ,, ,,	blpbaroe	probable
420	1 ,, ,,		*delete* not

(*Vol. XLVII, No.* 3, *March* 1958)

156	2 (from bottom)	$\omega_0 l_0$	$\omega_0 x_0$
156	1	$v =$	$v =$
168	24	0·1095	− 0·1095
168	25	$2{\cdot}5\times10^{-5}$	$-\ 2{\cdot}5\times10^{-5}$
169	1	137·5	137·05
171	4	bands	band

172, Table V, in column "Dissociation products" from the bottom 3rd line, for "*ab*" read "*aa*"

172, Table V, in column "Dissociation products" from the bottom 4th line, for "*bb*" read "*ab*"

191–195	Tamaraxetin	Tamarixetin

NOTICE TO AUTHORS

Scientific papers intended for publication in the *Proceedings of the Indian Academy of Sciences* can be accepted only when they are communicated by a Fellow of the Academy whose duty shall be to satisfy himself that such communications are fit to be read at the Meeting of the Academy and published in its *Proceedings*.

Papers should not ordinarily exceed fifty pages of foolscap. MSS. should be either typewritten or written in legible hand on one side of the paper. All papers should be carefully revised by the authors and should be absolutely in final form for printing. Position for text-figures should be indicated. Each paper shall conclude with a critical summary not exceeding 350 words.

Drawings, diagrams or other illustrations should be made on larger scale (preferably) twice the size than the ones in which they are intended to appear. They should be done in Indian ink on bristol board with lettering in pencil. Scale of magnification of camera lucida tracings should be indicated by the side of drawings. In certain special cases arrangements will also be made for monochrome lithographic and other colour plates. Reduction of illustrations desired should be indicated in pencil. Appropriate legends should accompany all drawings. Names of authors are to be marked in pencil on the left-hand corner of drawing sheets. Photomicrographs should be securely mounted with colourless paste.

All tables, quotations and footnotes which will be set hereafter (beginning from Vol. I, No. 2) in types smaller than the text, should be typewritten on separate sheets and placed with the text in proper sequence. Footnotes should be numbered in Arabic numerals.

References to literature in the text should be given, whenever possible, in chronological order, only the names of authors and years of publication, in brackets, being given. They should be cited in full after the summary, the authors' names following in alphabetical order. Thus,

Name or Names of author; Name of Journal (abbreviation) with a single underline; Year of publication; Number of Volume with a double underline, and lastly page. The following would be a useful illustration:—

Bergmann and Stather . . . . . Z. Physiol. Chem., 1926, 152, 189.

Two copies of slip-proof and wherever possible, a page proof for final revision will be sent to authors. All corrections are best made on the slip-proof which should be transmitted to the Office of the Academy. All proof corrections involve heavy expenses which would be negligible if the papers are carefully revised by the authors before submission.

Fifty free reprints including plates and with cover will be supplied for each paper. Additional copies can be supplied at cost on previous intimation.

Blocks appearing in the *Proceedings* will be available for purchase by their respective authors. Orders for the same should be sent along with the corrected proofs and in any case not later than one month after the date of publication of the paper. The price charged would be 25% of the actual cost of the blocks *plus* freight and despatching charges. If the blocks are reproduced in other journals or publications, due acknowledgment should be made in them to the *Proceedings*.

The original drawings and plates of blocks appearing in the *Proceedings* will be returned to such of the authors as may require them provided the cost of despatching such originals is borne by them.

CONTENTS

PAGE

The Optic Interference Figures of Amethystine Quartz—Part I . . . . . S. Pancharatnam 201

The Optic Interference Figures of Amethystine Quartz—Part II . . . . . S. Pancharatnam 210

The Factors that Affect Alkali Colour Reactions of Flavonols: A Study of Flavonols of Uncommon Types . V. K. Ahluwalia, N. R. Krishnaswami, S. K. Mukerjee, V. V. S. Murti, T. R. Seshadri and C. Venkataramani 230

Gravimetric Determination of Thorium and Its Separation from Uranium, Cerite Earths and Ceric Salts . . . G. M. Saxena and T. R. Seshadri 238

Heterocyclic Compounds. Part XIII. Synthetic Experiments in Furoquinolines . . . . . P. S. Raman 244

Effect of Methyl Orange on the Capacity of the Dropping Mercury Electrode . . . . . S. L. Gupta 254